Department of Mechanical Engineering

In-plane Tire Deformation Measurement Using a Multi-Laser Sensor System

Yi Xiong

Aalto University

DOCTORAL DISSERTATIONS

Aalto University publication series
DOCTORAL DISSERTATIONS 89/2016

In-plane Tire Deformation Measurement Using a Multi-Laser Sensor System

Yi Xiong

A doctoral dissertation completed for the degree of Doctor of Science (Technology) to be defended, with the permission of the Aalto University School of Engineering, at a public examination held at the lecture hall K216 of the K1 builiding (Otakaari 4) on the 3rd of June 2016 at 12 noon.

Aalto University
School of Engineering
Department of Mechanical Engineering
Vehicle Engineering

Supervising professor
Professor Kari Tammi, Aalto University

Thesis advisor
D.Sc. (Tech) Ari Tuononen, Aalto University

Preliminary examiners
Professor Annika Stensson Trigell, KTH Royal Institute of Technology, Sweden
Professor Igo J.M. Besselink, Eindhoven University of Technology, The Netherlands

Opponent
Professor Schalk Els, University of Pretoria, South Africa

Aalto University publication series
DOCTORAL DISSERTATIONS 89/2016

ISBN 978-952-60-6802-2 (printed)
ISBN 978-952-60-6803-9 (pdf)
ISSN-L 1799-4934
ISSN 1799-4934 (printed)
ISSN 1799-4942 (pdf)
http://urn.fi/URN:ISBN:978-952-60-6803-9

Unigrafia Oy
Helsinki 2016

Finland

441 697
Printed matter

Author
Yi Xiong

Name of the doctoral dissertation
In-plane Tire Deformation Measurement Using a Multi-Laser Sensor System

Publisher School of Engineering

Unit Department of Mechanical Engineering

Series Aalto University publication series DOCTORAL DISSERTATIONS 89/2016

Field of research Engineering Design and Production

Manuscript submitted 22 December 2015 **Date of the defence** 3 June 2016

Permission to publish granted (date) 14 April 2016 **Language** English

☐ **Monograph** ☒ **Article dissertation** ☐ **Essay dissertation**

Abstract

The interactions between tires and roads are basic mechanisms that alter the dynamic states of vehicles. A fundamental understanding of tire-road interactions is clearly demanded in tire design to achieve performance improvements. The emergence of various tire sensors provides an opportunity to make accurate measurement of the physical quantities that are involved in tire-road interactions.

This thesis aims to measure and analyze the in-plane deformation of rolling tires through its direct correlations with the steady-state in-plane tire forces. To date, there is no existing tire sensor that can measure both the tread and carcass deformations. A multi-laser sensor system has therefor been developed in the thesis to measure the in-plane deformation of different tire parts, including the tread, carcass, and inner liner.

Measurements on tread deformation were conducted on both passenger car and truck tires. A non-uniform tread deformation was observed in the measurement and was interpreted as follows: the asymmetric deformation in the longitudinal direction is a direct indicator of the rolling resistance and the non-uniform deformation in the lateral direction reflects the contribution of separate parts to the rolling resistance. The evolution and variation of tread deformations were investigated with different tire types, operational conditions, and tire states. The deformation of the carcass was first analyzed with the flexible ring tire model and then validated through tire sensor measurements. Coupled deformations of the tire carcass in the tangential and radial directions were observed. Indicators based on measured radial carcass deformations are proposed for the estimation of the in-plane tire forces. In addition, the partial inner contours were also measured for truck tires under static conditions for various inflation pressures and loads. The measurements can help tire designers to obtain optimum inner tire contours.

In summary, this thesis shows that the tire sensor can act as a powerful tool for tire research and development. The relations between the in-plane deformation and in-plane tire forces that have been obtained are useful in gaining an understanding of the physical mechanism of observed phenomena, e.g., the rolling resistance, and in the design of basic estimation algorithms, e.g., for the estimation of in-plane tire forces, which are important factors in the development of *green* and *intelligent* tires.

Keywords tire sensor, tire-road interactions, tire deformation, rolling resistance, tire force estimation

ISBN (printed) 978-952-60-6802-2 **ISBN (pdf)** 978-952-60-6803-9

ISSN-L 1799-4934 **ISSN (printed)** 1799-4934 **ISSN (pdf)** 1799-4942

Location of publisher Helsinki **Location of printing** Helsinki **Year** 2016

Pages 108 **urn** http://urn.fi/URN:ISBN:978-952-60-6803-9

This thesis is dedicated to the memory of my grandfather, Xiong Gan (1927-2011).

Acknowledgements

The research leading to this dissertation has been carried out in Vehicle Engineering Research Group at Aalto University, during the years 2012–2016. The major work was performed within the LORRY project which was funded by the European Community's Seventh Framework Programme (FP7/2007-2013) under grant agreement No. 314463. This work was also partially funded by the Doctoral School of Engineering, Aalto University. The support is gratefully acknowledged.

First and foremost, I would like to express my sincere gratitude to my instructor Dr. Ari Tuononen who has instructed this work. This dissertation could not have been completed without his inspiration and instruction. I am very grateful to my supervisor Prof. Kari Tammi for the guidance and encouragement to improve the quality of this dissertation. In addition, Prof. Matti Juhala and Prof. Petri Kuosmanen are also acknowledged for their support during the study.

I would like to thank to Prof. Annika Stensson Trigell and Prof. Igo J. M. Besselink for pre-examining this thesis and for providing valuable feedback. I feel honored that Prof. Schalk Els agreed to act as my opponent in the public defense of the dissertation.

I am indebted to many of my colleagues for creating a pleasant and dynamic work environment. Special thanks to our chief engineer Panu Sainio who always help me with his brilliant ideas to tackle practical problems during experiments. It is my great pleasure to study and work together with other PhD students in the group: Mona Mahboob Kanafi, Arto Niskanen, and Andras Kriston.

I am also grateful to the support that I have received from our technicians Pekka Martelius, Ari Nissilä, as well as our secretary Ritva Kähkönen.

Also I would like to thank all my dear friends in Finland, especially Hengda and his wife Chuqiao for the wonderful and memorable time which we have spent together.

Finally, I am deeply indebted to my father Zhemin and mother Jinlian for their unconditional love.

Leuven, April , 2016
Yi Xiong

Contents

List of Symbols

A	area of tire cross-section
A_{n1}	modal participation factor 1
A_{n2}	modal participation factor 2
B	carcass width
E'	storage modulus
E''	loss modulus
E^*	complex modulus
F_N	vertical force in the flexible ring tire model
F_x	longitudinal force applied on a tire
F_y	lateral force applied on a tire
F_z	vertical force applied on a tire from grounds
F'_z	vertical load applied on a tire
F_r	rolling resistance force
g_n	modal damping factor
h	carcass thickness
k_n	modal stiffness factor
k_v	equivalent tangential stiffness
k_w	equivalent radial stiffness
L_1	sidewall height
L_2	loaded radius
L_{offset}	mechanical offset
m_n	modal equivalent mass
M_r	rolling resistance moment
n	modal number

p_o	inflation pressure
R	tire radius
w	radial deformation of a tire element in the flexible ring tire model
w_{l_m}	mean radial deformation of tire carcass
w_{l_d}	difference between the mean measured deformation of the tire carcass before and after the contact
v	tangential deformation of a tire element in the flexible ring tire model
Z_{tread}	compressed tread thickness
θ	circumferential position of the in-tire sensor
ε_o	maximum strain of a rubber sample in a dynamical mechanical analysis
ε^*	strain in a complex notation of a rubber sample in a dynamical mechanical analysis
δ	loss angle of a rubber compound
ρ	tire density
σ_o	maximum stress of a rubber sample in a dynamical mechanical analysis
σ^*	stress in a complex notation of a rubber sample in a dynamical mechanical analysis
φ	circumferential position of a tire element in the flexible ring tire model
ω	excitation frequency in a dynamical mechanical analysis
Ω	rotating speed of tire

List of Abbreviations

ABS	Anti-Lock Braking System
ACC	Adaptive Cruise Control
ADAS	Advanced Driver Assistance Systems
CO_2	Carbon dioxide
C2C	Car to Car
C2I	Car to Infrastructure
FEM	Finite Element Model
LED	Light-Emitting Diode
LTS	Laser Tire Sensor
PSD	Position-Sensitive Detector
PVDF	Polyvinylidene Fluoride
RRC	Rolling Resistance Coefficient
R&D	Research and Development
REF	Ring on Elastic Foundation
SAE	Society of Automotive Engineers
TCOT	Tension Control Optimization Theory
TPMS	Tire Pressure Monitoring System
TTSP	Time-Temperature Superposition
ISO	International Organization for Standardization
ISP	Intelligent Speed Adaptation
WLF	Williams-Landel-Ferry
1D	One-dimensional
2D	Two-dimensional

List of Publications

This doctoral dissertation consists of a summary and of the following publications which are referred to in the text by their numerals.

Article I. Y. Xiong, A. Tuononen. A Laser-based Sensor System for Tire Tread Deformation Measurement. Measurement Science and Technology, 25(11), 11503, pp.1-9, 2014. DOI: 10.1088/0957-0233/25/11/115103

Article II. Y. Xiong, A. Tuononen. A Multi-Laser Sensor System to Measure Rolling Deformation for Truck Tyres, Accepted to International Journal of Vehicle Performance. In press.

Article III. Y. Xiong, A. Tuononen. Rolling Deformation of Truck Tires: Measurement and Analysis Using a Tire Sensing Approach. Journal of Terramechanics, 61, pp. 33-42, 2015. DOI: 10.1016/j.jterra.2015.07.004

Article IV. Y. Xiong, A. Tuononen. The In-plane Deformation of a Tire Carcass: Analysis and Measurement, Case Studies in Mechanical Systems and Signal Processing, 2, pp. 12-18, 2015. DOI :10.1016/j.csmssp.2015.09.001

Author's Contribution

The author wrote the draft of manuscripts for Articles [I]-[IV], and edited the final version based on the inputs from Dr. Ari Tuononen. In Articles [I]-[III], the author implemented the research plan defined by Dr. Ari Tuononen. For Article [IV], the author defined the research plan, and implemented the plan with the help of Arto Niskanen in the experiments. For all articles, the measurement setup and analysis procedure presented in this work were developed by the author and the results were interpreted together with Dr. Ari Tuononen.

1. Introduction

1.1 Background

The pneumatic tire has been an essential automotive component since its inception and plays a significant role in the safety, mobility, handling, comfort, and fuel economy of vehicle systems. In the year 2013, about 263.6 million tire units (for cars and trucks) were sold in the European Union, which represents about 20% of the global tire market [1]. In the next decade, it is anticipated that the size of global market will continue to experience consistent growth because of rapid increases in vehicle sales in the emerging economies. Improvements in the performance of tires, even minor ones, can contribute significantly to resolving challenges in the transport sector, such as global warming, air pollution, and the energy crisis. To promote more sustainable mobility, the development of modern tires is driven towards a resource-efficient direction, in addition to fulfilling the conventional design requirements, which are durability and safety. Regional tire labeling systems are published or being introduced by local regulators worldwide, e.g., the European Union, the United States, Japan, South Korea, and China, to increase public awareness on tire performance, including the rolling resistance, wet grip and, in some cases, also rolling noise [2].

The tire influences vehicle fuel economy and CO2 emissions mainly through its rolling resistance performance. It has been established that the rolling resistance of tires can account for as much as 17-21% of the total fuel consumption of ground vehicles, while the contributions are even higher for heavy-duty vehicles [3]. From a broader perspective, 58% of the global oil consumption and about 20% of total global greenhouse gas emissions come from the transport sector. Lowering the rolling resistance of tires is listed as a key issue to investigate in both the European Commission White Paper for Transportation [4] and the European Green Car Initiative roadmap [5] to achieve the EU's long-term targets, including improving transport efficiency by 50% by 2030 and reducing CO2 emissions in transport by 60% by 2050.Tire manufactures have made considerable efforts to reduce the rolling resistance through the development of new tread patterns, tire structures, and compounds. As a direct consequence, the rolling resistance performance of modern radial tires was greatly improved by introducing innovative technologies such as silica filler, weight reduction, and functionalized polymers. In addition, it is claimed in studies [6]–[8] that every reduction by 10% in the rolling resistance promises a 1 to 2% increase in the fuel economy.

For electric and hybrid cars, the reduction of the rolling resistance is more important in increasing the driving range per charge, as a result of improved energy efficiencies in the other vehicle parts. This market segment, with especially rigorous requirements in terms of rolling resistance performance, has been established and products such as Michelin Energy E-V and Continental eContact have already been released to the public. Those tires adopted designs with low weights, low aspect ratios, and large radiuses to minimize the tire deformation during contacts. Such design leads to a 20-30% improvement in rolling resistance performance compared to conventional tires, and the energy saved corresponds to about a 6% improvement in the travel range.

In addition to a 'green' tire with lower fuel consumption and CO_2 emissions, an 'intelligent' tire with the ability to provide tire-road information is also desired. It is expected that the electrification of a tire can transform the tire from a passive vehicle component into a proactive component that is better suited to future vehicle systems. Being able to capture information about tire-road interactions, especially tire forces and moments, will be beneficial for many advanced driver assistance systems (ADAS), including adaptive cruise control (ACC), anti-lock braking systems (ABS), intelligent speed adaptation (ISP), etc. Meanwhile, the advanced warning function regarding challenging driving conditions, such as driving on wet and slippery roads, can be very useful in assisting drivers to choose a safe driving strategy, and therefore preventing traffic accidents. In future, it will be possible to share the real-time road information among drivers, road maintainers, and other stakeholders through car-to-car (C2C) and car-to-infrastructure (C2I) communication.

Fundamental understandings of tire-road interactions are essential in the development of 'green' or 'intelligent' tires. The vehicle, tire, and road form a coupled system and need to be studied together because of their mutual influences. The interactions between tires and roads are basic mechanisms that alter the dynamic states of a vehicle. On one hand, the interactions develop the desired tire forces and moments to support vehicle weights and to implement drivers' commands to vehicles, such as braking, accelerating, and cornering. On the other hand, interactions such as the aquaplaning, abrasion, and rolling resistance lead to degradations of vehicle performance in terms of safety, durability, and economy. However, it is not easy to obtain or accurately measure information regarding tire-road interactions, because the specific location for sensor operations has a harsh environment and experiences disruptive impacts. The harsh environment inside the tire cavity, with large temperature variations (from the ambient temperature to 20 degrees higher), high accelerations (at 200 km/h, acceleration up to 3000 standard gravity), and large deformations (a strain up to 0.3 during the contact), requires reliable, low-weight, and modularized sensors.

Over the past decade, the emergence of various tire sensor systems has provided a foundation for a paradigm shift using experimental measurements in studies of tire-road interactions. One well-known example of tire state monitoring systems is the tire pressure monitoring system (TPMS), which is widely installed into mass-produced vehicles and legislated in the European

Union and the United States. Additionally, more physical quantities, such as the dynamic contact stresses and accelerations on inner liners, can be measured nowadays. This allows the theoretical analysis in the early phase of design through such means as the finite element model (FEM) to be experimentally validated and the design process greatly shortened. New opportunities are provided by tire sensor systems to revolutionize the conventional 'build-and-test' mentality that was adapted in the tire development process and led first to the building of different variations and then to testing to decide performance directions [9]. Furthermore, it provides a way to measure characteristics of final tire products which is difficult to predict because of their complex construction and manufacturing process.

One important tire characteristic to measure is the in-plane deformation of a tire which is a direct result of the in-plane tire forces applied to the complex structure of a tire. Systematic measurements of the in-plane deformation of tires can assist tire designers to understand the physical mechanism of observed phenomena, e.g., rolling resistance, and to design basic estimation algorithms, e.g., for the estimation of tire forces, which are important aspects of the development of 'green' and 'intelligent' tires. Thus, an important motivation in this thesis is to measure in-plane tire deformations using a recently developed multi-laser tire sensor system. It attempts to provide some basic understandings about the in-plane tire deformation on the basis of field measurements, in order to facilitate improvements in tire performance.

1.2 Aims and scope

Taking into account the direct link between the in-plane tire deformation and tire performance discussed above, the overarching purpose of this research is to **measure** and **analyze** in-plane deformations of a tire, especially the tread and carcass part, under steady-state in-plane tire forces. Currently, there is no existing sensor system available to measure the complete tread deformation. As a starting point, the first task of this thesis is to **develop a multi-laser tire sensor system** which is able to measure **deformations in the tread and carcass parts** of tires. Once the tire deformations have been measured, their direct links to tire performance need to be identified to fill the knowledge gap which has not been explored previously. Therefore, the second task is to interpret the measured physical quantities and find their links to specific aspects of **tire performance**, such as the **rolling resistance**, and **in-plane tire forces**. On the basis of the proposed correlations between the tire deformations and performance, it is worthwhile to study their **applicability** to different tires with different states, e.g., in-service wear. In addition, another task is to examine the **evolution** and **variation** of tire deformations under different operational conditions including the vertical force, inflation pressure, and rotational velocity. Finally, the research focuses on the feasibility of utilizing carcass deformation measurements for the **estimation of in-plane tire forces**.

1.3 Scientific contributions

The research presented in this thesis brings new knowledge about in-plane tire deformation to studies of tire-road interactions. The deformations of different tire parts, including the tread and carcass, were measured with a multi-laser tire sensor system that was developed in the thesis. Measurements were conducted on different tire types, both passenger car and truck tires, and different tire states, both new and used tires, and under different operational factors, such as the vertical force, inflation pressure, and rotational velocity. The work contributes to the advancement of this field from the following aspects.

- A multi-laser in-tire sensor system including both one-dimensional (1D) and two-dimensional (2D) versions has been developed to measure in-plane tire deformations. With this novel instrument, three physical quantities, namely the tread and carcass deformations, and inner contour of tire were obtained in measurements of a passenger car tire and truck tires. (in Article [I] and Article [II])

- The effects of the vertical force, inflation pressure, and rotational velocity on the tread and carcass deformation were quantified experimentally. (in Article [I] and Article [III])

- For tread deformation measurements, asymmetric patterns were observed in both the longitudinal and lateral directions. The asymmetric deformation in the longitudinal direction is linked to the rolling resistance performance of tires. In the lateral direction, a load shift effect of the asymmetric deformation was found when the new tire was under an increasing load. (in Article [I] and Article [III])

- For carcass deformation measurements, coupled deformations in the radial and tangential directions were observed. The radial deformation is influenced by both the vertical and longitudinal forces. Simple indicators based solely on the radial deformation of the tire carcass are proposed to estimate the in-plane tire forces. (in Article [IV])

2. State-of-the-art

2.1 Tire mechanics

The pneumatic tire is essentially a doubly-curved and multi-layered structure made from rubber-cord composites [10], [11]. The space between the tire and rim forms a cavity with pressurized air during the operation. The tire interacts with roads to serve different functions for vehicle systems: to support vehicle loads, to provide mobility, and to absorb road irregularities. In tire design, different rubber compounds are used in separate tire parts, from the outer tread to the inner liner, in order to maximize tire performance within aforementioned functions. Reinforcing materials such as tire cords and bead wires are constructed within a complex structure to provide strength and stability to the tire carcass. It is worth noting that terms such as tread, carcass, and inner liner are defined in tire mechanics to represent specific tire parts. However, the terminology is not systemically defined and consistently used across different literatures and therefore an illustration for the terms used in this thesis is presented in Figure 1.

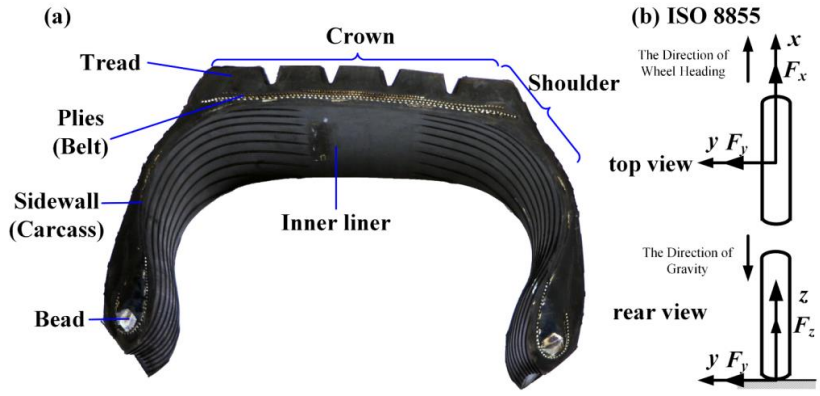

Figure 1 Illustration of (a) tire structure and nomenclature and (b) the Cartesian coordinate system according to the ISO 8855.

The Cartesian coordinate system for tire forces used in this thesis is defined according to the ISO 8855. The x- axis points toward the heading direction of a wheel, the z- axis points toward the opposite direction of the gravity vector, and the direction of the y- axis is determined by the right-hand rule. The coordinate

system of the flexible ring tire model is an exception that the *z*- axis points toward the direction of the gravity vector, as it is widely used in the literature.

2.1.1 Rubber compounds

Natural or synthetic rubber, mixed together with other additives such as fillers and agents, forms the rubber compound which is the major material (about 80-90%) used in tires [10]. Rubber compounds are viscoelastic materials which have a combined mechanical behavior that is partly viscous and partly elastic. The hysteresis property of tire rubber plays a key role in tire design because of its effects on both vehicle handling and rolling resistance performance.

The viscoelasticity of a rubber compound is typically characterized through dynamic mechanical analysis (DMA), in which a periodical excitation stress (e.g., sinusoidal excitation) is applied to the sample and its response strain is measured, or vice versa in some cases. As a result of the viscoelastic behavior, a time delay can be observed in the response after each excitation stress. To mathematically describe such behavior, the excitation stress with a frequency ω and corresponding strain can be expressed in a complex notation as

$$\begin{aligned} \sigma^*(t) &= \sigma_0 e^{\omega t i} \\ \varepsilon^*(t) &= \varepsilon_0 e^{(\omega t+\delta)i} \end{aligned} \tag{2.1}$$

where σ_0 and ε_0 are the maximum stress and strain, respectively. δ is the phase lag between the stress and strain; the value is zero for pure elastic materials and $\pi/2$ for fluids. The complex modulus E^* is the ratio between $\sigma^*(t)$ and $\varepsilon^*(t)$.

$$E^* = \frac{\sigma^*(t)}{\varepsilon^*(t)} = \left(\frac{\sigma_0}{\varepsilon_0}\right) e^{\delta i} = \frac{\sigma_0}{\varepsilon_0}\cos\delta + i\frac{\sigma_0}{\varepsilon_0}\sin\delta = E' + iE'' \tag{2.2}$$

where the storage modulus and loss modulus are defined as $E' = (\sigma_o/\varepsilon_o)\cos\delta$ and $E'' = (\sigma_o/\varepsilon_o)\sin\delta$, respectively. The storage modulus measures the elastic component and the loss modulus measures the viscous component of viscoelastic materials. As shown in Figure 2 , the following relation can be found from the definition of E'' and E':

$$\tan\delta = E''/E' \tag{2.3}$$

where $\tan\delta$ is also called the loss factor or loss tangent.

The loss factor is an indicator to quantify the viscoelastic behavior of rubber compounds. A compound with a low loss tangent value, which dissipates less energy during cyclic deformations, is clearly demanded in the development of tires with a low rolling resistance. However, it has generally been accepted that a higher loss tangent leads to better vehicle handling performance, such as high wet traction and a better frictional grip. Thus, a simple reduction of the loss factor cannot improve overall tire performance because of its adverse influences

on other aspects of tire performance. This trade-off in tire design can be explained with an extreme case: a tire cannot be constructed with purely elastic materials since although it would have a minimum rolling resistance it could not provide enough traction. Furthermore, the viscoelastic behavior of rubber compounds is dependent on a number of factors, of which the most important ones are temperature, frequency and strain amplitude.

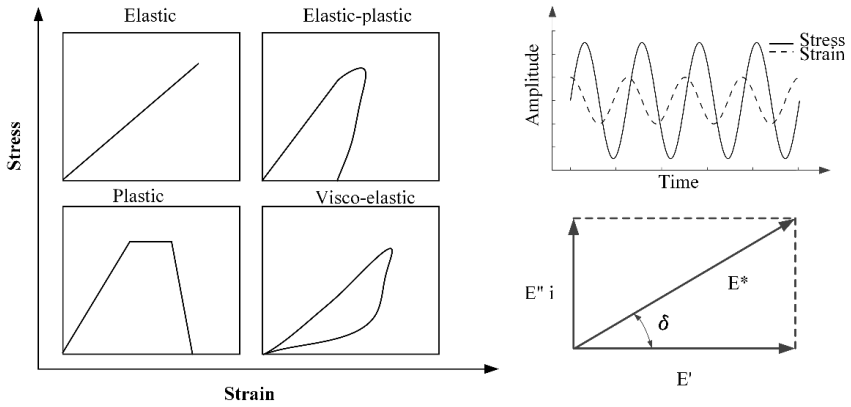

Figure 2 Viscoelastic behavior of rubber compounds.

The mobility of chains and segments in rubber compounds is distinct at different temperatures [12]. Hence, the temperature has strong influences on the mechanical characterization of the rubber compound, and ultimately on tire performance. For instance, it has been established that the behavior of a rubber compound around its glassy transient temperature has a strong influence on the abrasion resistance. In this temperature region, the rubber compound has a high modulus and a maximum loss angle, as shown in Figure 3. Moreover, the skid behavior and traction of the tire are correlated to the loss angle of the rubber compound at the temperature range from 0°C to the ambient temperature. In the tire industry, the rolling resistance performance of a tire is optimized on the basis of the loss angle of the rubber compound around 60°C and a low value of the loss angle is desired. With a further increase in the temperature, rubber compounds start to degrade and reach the limits of driving safety. In this temperature region the loss angle indicates the heat buildup properties [13] and its value is expected to be lower.

The excitation frequency influences the viscoelastic behavior of a rubber compound in a similar manner to the temperature. According to the time-temperature superposition principle (TTSP) or Williams-Landel-Ferry (WLF) model, an increasing temperature and a decreasing excitation frequency have the same influences on the dynamic response of rubber compounds. In terms of the energy dissipation, two frequency ranges which correspond to distinct physical mechanisms receive special attention [14]. First, the main excitation frequency for a free-rolling tire ranges from 10 to 10^3 Hz, which is caused by cyclical deformations caused by contact with roads. In contrast to that, for a tire that is sliding, the main contact excitation frequency will be increased to the

regime from 10^4 to 10^6Hz as a result of the pulsating forces generated by road asperities.

In addition, the viscoelastic behavior of a rubber compound is also amplitude-dependent, e.g., the dynamic modulus decreases with increasing amplitude. This dependence is especially prominent for compounds with a large proportion of fillers subjected to moderate amplitude and low to moderate frequency [15].

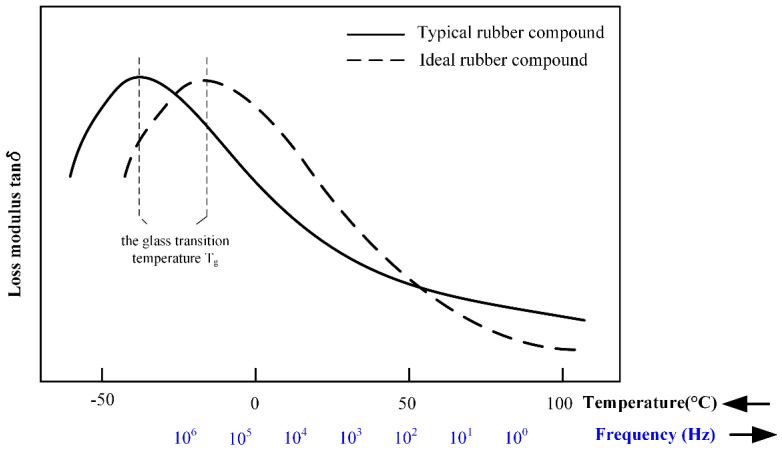

Figure 3 Loss moduli of typical and ideal rubber compounds against different temperatures and frequency ranges.

In previous tire developments, tires with optimum performance were obtained by shifting the characteristic curve of the rubber compound. This leads to an improvement of certain aspects of the performance of the rubber compound by moving the curve in the desired direction, but it also sacrifices other performance by moving the curve to the undesired direction. This will result in a trade-off in tire design among different tire performance. In general, the hysteresis property of a rubber compound is expected to be maximized to increase frictional grip for vehicle braking and acceleration and to be minimized to reduce the rolling resistance and improve the fuel economy of vehicle systems. This dilemma is nowadays partially resolved by exploiting the viscoelastic properties of rubber through the development of polymers and compounding ingredients with the desired dynamic mechanical properties (see Figure 3), which behaves differently at different temperatures and frequency regimes of tire operation.

2.1.2 In-plane tire forces

As discussed before, one primary task of tires is to provide mobility for the vehicle to move forwards or backwards. For a wheel moving in a straight direction, free body diagrams of the in-plane tire forces applied to the driven and non-driven wheels are shown in Figure 4. If the wheel is in a free-rolling case, the in-plane forces include the vertical force from a wheel hub F_z, the vertical force from grounds F'_z, and the driving force F_d (for a non-driven wheel) or the driving moment M_d (for a driven wheel). If longitudinal slips of the tire

are in present, the corresponding traction force F_x or the vehicle drag force F_{drag} (for a driven wheel) is added respectively. The governing equilibrium equations are therefore written as:

- for a non-driven wheel

$$\begin{aligned} &force: \begin{cases} F_x = F_d \\ F_z = F_z' \end{cases} \\ &moment: F_z \cdot a - F_x \cdot R = 0 \end{aligned} \tag{2.4}$$

- for a driven wheel

$$\begin{aligned} &force: \begin{cases} F_x = F_{drag} \\ F_z = F_z' \end{cases} \\ &moment: F_z \cdot a + F_x \cdot R = M_d \end{aligned} \tag{2.5}$$

This thesis limits its scope to in-plane tire deformations caused by steady-state in-plane forces, namely the vertical forces (vertical forces) and the longitudinal forces (the rolling resistance force, traction force, and braking force).

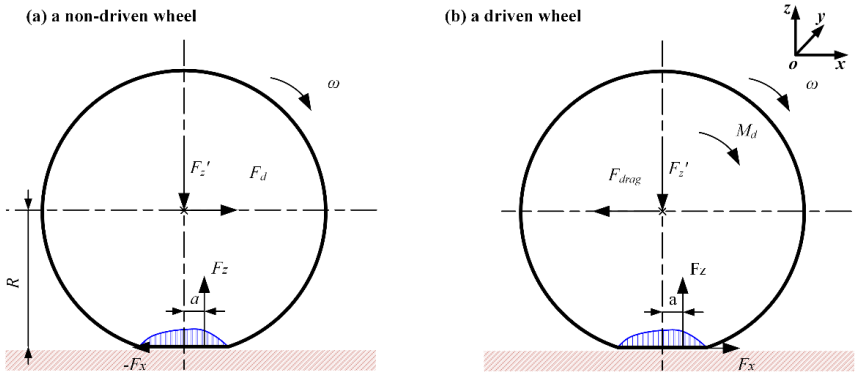

Figure 4 In-plane tire forces applied to (a) a non-driven wheel and (b) a driven wheel.

The rolling resistance is a universal characteristic of rolling objects to resist the rolling motion in the presence of all conditions. The rolling resistance is defined as the loss of energy (or energy consumed) per unit of distance traveled and the unit is therefore either Joule/Meter or Newton in different international standards, for instance the ISO 28580 and SAE J1269 standards. This definition reflects the fact that the rolling resistance is essentially an energy dissipation process rather than a physical force, though the unit can be Newtons. The reason why the rolling resistance is expressed as a pseudo-force, which has no applied point, is due to the practice that the tire spindle force, which is equivalent to the rolling resistance, is typically being measured instead of the energy dissipated during traveling. Several tire models based on the energy dissipation mechanism have been proposed recently, as shown in [16]–[18].

In the tire labeling system, the rolling resistance coefficient (RRC), as the ratio of the rolling resistance to the vertical force on the tire, is used to compare the rolling resistance performance across different tires. However, the base assumption of using RRC, which is a near-linear relationship between the rolling resistance and vertical force, is not always valid, especially for conditions with large tires and heavy loads, according to the studies in [19]. Typical values for the rolling resistance coefficient are in the ranges from 0.6%-1.5% for new passenger car tires (C1 class tires), and 0.4%-1.2% for new heavy truck tires (C3 class tires).

In terms of energy losses, there are three physical mechanisms involved, excluding the parasitic losses such as the bearing friction. The main cause is the cyclic deformation caused by contact with roads and two secondary mechanisms include micro-slippages at the tire-road interfaces and aerodynamic drag. Moreover, the cyclic deformation of the tread by the road can be further classified into: compression, shear, and bending deformations.

In modern radial tire design, the rolling loss caused by the bending deformation of the tread is minimized through the application of more flexible tread patterns. The contribution of cyclic compression of the tread to the rolling resistance loss can be explained as follows. The tread blocks experience loading and unloading processes during their contact with the road. As a result of the viscoelastic behavior of the rubber compound, the stress is greater in the loading process (in the leading half) than in the unloading process (in the trailing half) for the same strain. This results in an asymmetric normal stress distribution in the contact patch, which has a shifted equivalent force located in the leading half of the contact patch, as shown in Figure 5, and the equivalent force resists the rolling motion of the tire. A similar mechanism can also be found in the shear deformation of tread part and results in a horizontal force that resist the rolling motion of the tire. However, the shear deformation depends strongly on the tread compression as a result of the incompressibility of the tread compounds (Poisson's ratio≈0.5). In addition, the tread compression also affects the tire-road friction, which is an important factor in the shear deformation. Hence, this thesis focuses on the measurements of the compression of the tire tread using the tire sensing technology is discussed in the next subsection. The deformation mentioned in this thesis refers to the compression in the vertical direction.

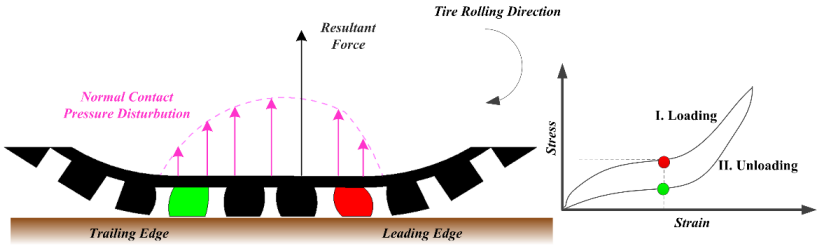

Figure 5 Mechanism of tire rolling resistance due to compressions: the tread block within the leading half (red) is in the loading states and the tread block within the trailing half (green) is in the unloading process.

One primary function of tires is to develop the desired forces to alter the dynamic states of vehicles. In contrast to the rolling resistance force, a better understanding of the in-plane tire forces has been gained. Different tire models can be found covering from the (quasi-) steady to transient states, and from in-plane to out-of-plane behavior [20]. In addition, the characteristic of tire forces are greatly influenced by tire inflation pressure and tire wear as shown in [21], [22].

The tire carcass is the only transmission path for tire forces and moments between the contact patch, where the forces and moments are developed, and the rim, where the forces and moments are eventually applied to the vehicle body. One direct effect of the transmission of the forces and moments is the deformation of carcass in three directions. In the equatorial plane of the tire, the deformations mainly include radial deflection and tangential distortion. It is therefore of great interest to investigate the relationship between the in-plane tire forces and in-plane deformation, which can form the basis of the algorithm for the development of the tire sensor.

2.1.3 Flexible ring tire model

The flexible ring tire model, one of the Ring on Elastic Foundation (REF) models, is an important tool for simulating and analyzing the deformation of a tire carcass. It is based on the observation that a tire behaves in a similar way to an elastic ring under the influence of excitation forces at a low frequency range of 0-300 Hz [23]–[25]. Thus, the flexible ring tire model has been widely used to investigate in-plane tire behavior [26]–[28] . In this model, a tire is described as an elastic ring with parallel springs connected, in both the radial and tangential directions, to the rim, as shown in Figure 6 (a). For tire-road contacts, a single-point contact model for the vertical force F_N and longitudinal force F_x is used instead of a distributed contact model. This is an appropriate simplification for measurements conducted on a curved surface, since the contact patch length is shorter than on a flat surface and the contact forces are closer to the contact center.

Because of the high extensional stiffness of the modern radial tire, the middle surface of the tire carcass is assumed to be inextensible [26]. Hence, the radial deformation w and tangential deformation v of the tire carcass in a circumferential position φ are governed by the following relation:

$$w(\varphi) = -\partial v(\varphi)/\partial \varphi \tag{2.6}$$

The deformation of the ring is expressed in the modal expansion form, which assumes that the response of a complex linear multi-degree-of-freedom (MDOF) system can be represented as a weighted summation from the 1st mode shape until the ith mode shapes of the system.

The radial deformation w and tangential deformation v for the tire carcass read:

$$\begin{aligned} v(\varphi) &= \sum_{n=1}^{i} \left[A_{n1} F_x \sin(n\varphi) + A_{n2} F_N \cos(n\varphi) \right] \\ w(\varphi) &= \sum_{n=1}^{i} \left[-nA_{n1} F_x \cos(n\varphi) + nA_{n2} F_N \sin(n\varphi) \right] \end{aligned} \tag{2.7}$$

where the pre-tension force in the carcass:

$$\sigma_\theta^o = p_0 bR + \rho A R^2 \Omega^2 \tag{2.8}$$

modal equivalent mass:

$$m_n = \rho A (1 + n^2) \tag{2.9}$$

modal damping factor:

$$g_n = -4\rho A n \Omega \tag{2.10}$$

modal stiffness factor:

$$\begin{aligned} k_n = (EIn^2 / R^4 + \sigma_\theta^o / R^2)\left(1 - n^2\right)^2 - p_0 b\left(1 - n^2\right) / R + \\ k_v + k_w n^2 - \rho A\left(1 + n^2\right)\Omega^2 \end{aligned} . \tag{2.11}$$

In addition, modal participation factor 1:

$$A_{n1} = 1 / \pi \sqrt{\left(m_n n^2 \Omega^2 + g_n n \Omega - k_n\right)} \tag{2.12}$$

and modal participation factor 2:

$$A_{n2} = nA_{n1} . \tag{2.13}$$

As shown in Figure 6 (b), the flexible ring tire model can be used to simulate and investigate the impact of tire forces on the contour and deformation of the tire carcass. Because of the inextensibility of the tire carcass, it is observed that the in-plane deformation has the following two features. First, the radial and tangential deformations of the tire are coupled. Moreover, the part of the tire which is not in contact with the road is also deformed and is influenced by the deformation of the tire in the contact zone.

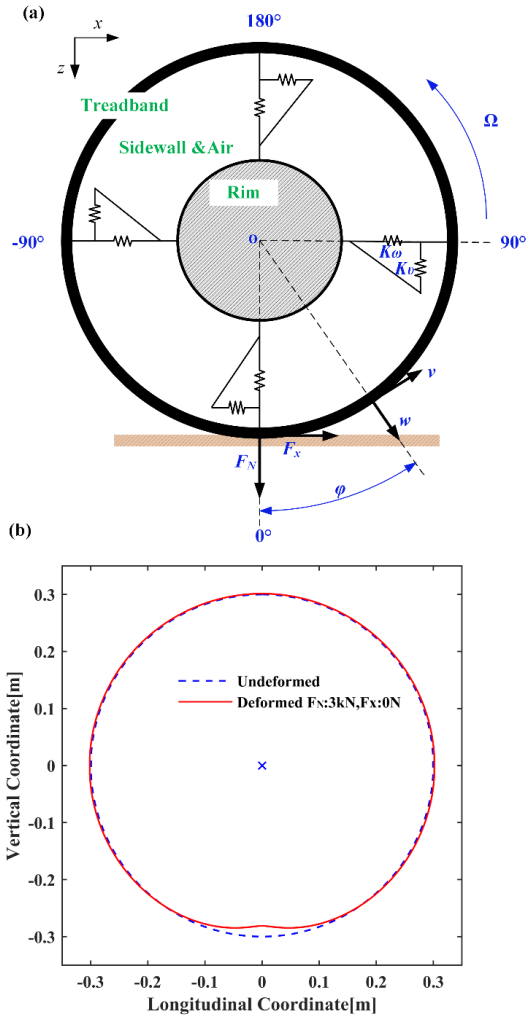

Figure 6 (a) The flexible ring tire model; (b) simulated tire contours from the flexible ring tire model (inflation pressure: 2.2 bar).

2.2 Tire sensing technology

The past two decades have witnessed a remarkable evolution of tire sensor systems since the concept first arose through the Darmstadt tire sensor in 1988 [29]–[31]. The tire sensor system provides direct measurements of tire operating states, such as the acceleration, deformation, strain, temperature, and inflation pressure. The measured information is then used in various applications, which can be categorized into the following two fields:

- to improve the design of tires in the research and development (R&D) process, and;
- to upgrade the performance of vehicle control systems.

In this thesis, Articles [I]-[III] deals with the first application area and Article [IV] represents a case study in the second application area.

Measurements of tire states can take place either inside or outside a tire. Most existing tire sensor prototypes, including the system that will be presented in this thesis, belong to the category of in-tire sensing methods. In addition, applications have also been shown with sensor systems located in places outside tires, such as the suspension, wheel, and wheel bearing, which provide indirect measurements of tire states. Those methods are suitable for estimations of tire forces and moments, however, they are not suitable for examining the fundamental mechanisms of tire-road interactions, such as aquaplaning and rolling resistance, as the role of a tire acts as a filter between the tire-road contact and the sensor. In-tire sensors, which are closer to the tire-road contact, provide more accurate outputs and quick responses.

The major reported sensor types used for in-tire sensing methods include accelerometers, optical sensors, strain sensors, and polyvinylidene fluoride (PVDF) sensors. A brief comparison of major tire sensors in terms of accuracy, durability, cost, and influence on tire performance is presented in Table 1. Strain sensors are low-cost sensors but have deboning problems. PVDF sensors have a good measurement accuracy but are very sensitive to temperature changes. Hall sensors need to be installed inside tires and therefore have low scalability for the mass production. Recently, increasing research activities have focused on applications with accelerometers and optical sensors (see Figure 7). With a high overall performance, accelerometers have been used in different applications with a promising future. In addition, optical sensors with a high measurement accuracy are also widely used as tire sensors. However, the high cost and power consumption limit their application areas mainly to R&D. In addition to those sensor prototypes which have demonstrated their feasibility on tires in real operating conditions, other sensors have also been documented which have potential for tire-sensing applications.

Table 1 comparisons of major tire sensors (* H= high potential, M=middle potential, and L=low potential)

Sensor Types	Accuracy	Durability	Cost	Influence on tire	Applicability R&D/ Production
Accelerometer	M	H	M	M	H/H
Optical Sensor	H	H	H	L	H/M
Strain Sensor	M	L	L	M	M/L
PVDF	M	L	M	M	M/L
Hall Sensor	M	M	M	H	M/L

The deformation of each tire part has a unique effect on tire performance. Therefore, tire sensors have been developed to measure deformations of specific parts, such as the following:

- sidewall deformation measurement [32], [33];
- tread deformation measurement [34];
- footprint dynamic state measurement [35]–[38], and
- footprint static states measurement [39].

The tread is the only part of the tire that comes into contact with the road during normal driving and therefore it has a significant impact on the performance of tires, such as the traction, abrasion, and rolling resistance. Measurements of the tread deformation can enhance the understanding of tire-road interactions. Thus, one primary objective of this thesis is the measurement and interpretation of tread deformation measurements.

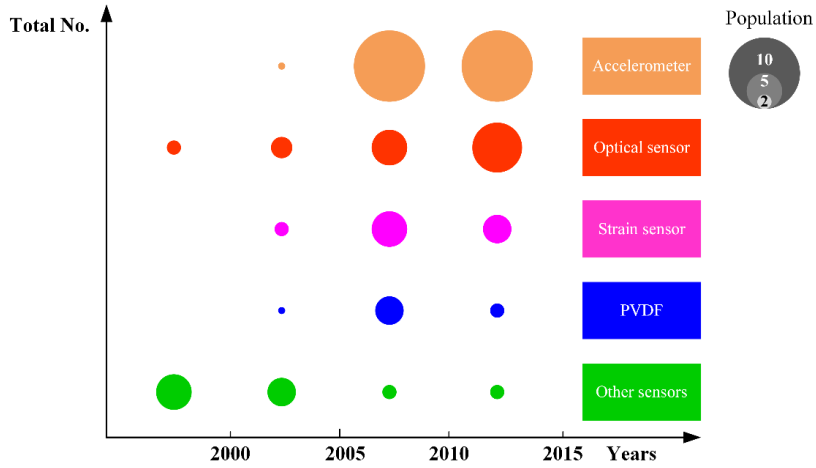

Figure 7 A summary of research prototypes of tire sensor systems.

Previous attempts to measure tread deformation are various [34], [40]. One well-known example is the Darmstadt tire sensor, as shown in [34].In this tire sensor, an array of Hall sensors was used to detect the position of a permanent magnet embedded in a tread element, and therefore to measure a partial deformation of the tread element. The horizontal deformations are estimated on the basis on differential signals between two arrays of Hall sensors in the *x*- and *y*- directions. Meanwhile, the deformation in the *z*- direction is obtained through the sum of the measurements from all the Hall sensors. The sensor performance is mainly influenced by the sensitivity of the cross magnetic Hall field, the size of the magnet, and the distance between the magnet and the Hall sensors. More importantly, the sensor only measures a partial deformation of the tread element in a sandwich structure. However, the complete tread deformation measurement is required to study tire-road interactions, particularly the rolling resistance. Thus, an additional tire sensor system with an ability to measure the complete tread deformation is needed.

For tire deformation measurements, optical sensors are widely used because of their high-accuracy measurements and capabilities to operate in harsh environments. In this non-contact and non-destructive method, sensors are fixed to the rim and not in contact with the tire being measured. In other words, the added sensor system has no influence on the mechanical characteristics of the tire and the inconvenience associated with tire replacements is avoided. Typical optical sensors used in tire sensing applications can be categorized into three groups: position-sensitive detectors (PSD) [41]–[44], lasers [33], and cameras [45], [46].

The cavity of a tire offers a unique environment for optical sensors. On one hand, the closed space protects the sensor from contamination, such as dust and water from the outside environment. On the other hand, while the dark environment ensures that the light disturbance is minimal, it also requires additional light sources for optical measurements. In earlier prototypes [41]–[43], systems based on a PSD combined with light-emitting diodes (LEDs) were demonstrated to measure carcass deformation. LEDs, which act as light sources, were glued to the inner liners of tires and positioned facing towards the PSD, which was fixed to the rim. Lights were focused through a lens to a light spot and projected onto the active areas of the PSD. The detected light spot position can therefore be used to determine LED positions caused by tire deformations. With a similar principle, systems based on a camera with an LED were used to measure the same quantities [44]. For better measurement reproducibility, a one-dimensional laser triangulation sensor, instead of the PSD and LED system in [41]–[43], was later used in [33] to measure the radial carcass deflection of a rolling tire at a normal driving speed and under complex driving conditions such as soil deformation and aquaplaning. The in-wheel integration design for the optical sensor in[33], [41]–[43] forms the basis for this thesis.

3. A multi-laser based tire sensor system

The multi-laser based tire sensor system is a basic tool developed in this thesis to measure the in-plane tire deformation. This section briefly presents the system structure and methodology of the tire sensor system that was developed.

3.1 System structure

An in-tire integration solution for optical measurements of the deformation of the tire carcass was demonstrated in a series of tire sensor prototypes developed at Aalto University. In a recent study [33], a one-dimensional laser tire sensor (LTS) system was developed to measure carcass deflections in a realistic environment and also under complex driving conditions, including soil deformation and aquaplaning. To measure tread deformations, the LTS system was extended in Article [I] by introducing an external spot-type laser sensor, as shown in Figure 8. This multi-laser based tire sensor system (1D) is able to measure the deformations of a tread element on passenger car tires during rolling. In addition, it still preserves the ability to measure carcass deformations in the radial direction, which is demonstrated in Article [IV]. Although giving promising results, the 1D tire sensor system has the inherent limitation that measurements are carried out on one spot of tread in the cross-section of the tire, but the tread deformation is not uniform along the cross-section of the tire. To extend the capability of the system to measure tread deformations over a wider area of the cross-section of the tire further, a 2D tire sensor system, which has an identical methodology to the 1D system, was therefore developed (see Figure 9) for measurements with truck tires in Article [II].

The multi-laser system consists of two laser triangulation sensors and an optical encoder. One laser sensor (the in-tire sensor) measures the tire deformation inside the tire cavity; meanwhile, the other one (the external sensor) measures the tire deformation outside of the tire, as shown in Figure 9. The dynamic loaded radius (wheel rotating axis distance from the road) can be measured directly from the external laser sensor (Keyence LK-H150). This sensor was fixed to a rigid mechanical support attached to the stator part of a slip ring. Hence, the position of the external laser is stationary about the rotating axle while a tire is rolling.

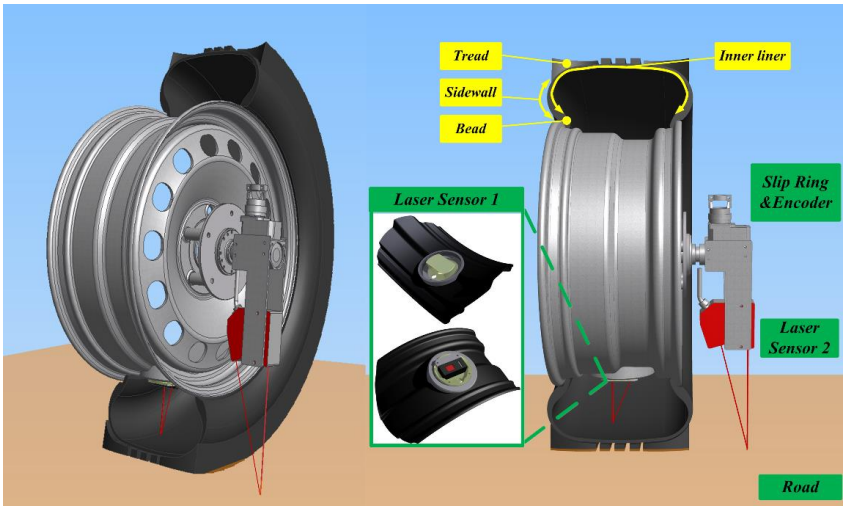

Figure 8 The tread deformation measurement system (1D version).

The in-tire laser sensor, which is the core sensor within the system, measures the distance from the rim to the inner liner. In the 1D and 2D versions, respectively, two different laser sensors, a Keyence IL-065 and Keyence LJ-V7300, were used as the in-tire sensors. Moreover, both laser sensors adapt the laser triangulation principle and the large dynamic range of the sensors allows measurements of objects such as tire rubber with weak reflections.

All the measurement units used in the system are industrial level sensors with high accuracies. According to the manufacturers' specification, the repeatability for the external laser sensor (Keyence LK-H150) is 0.25 μm. In addition, the repeatabilities for the in-tire laser sensors are 2 μm (1D laser, IL-065) and 5 μm (2D laser, LJ-V7300), respectively.

The in-tire laser sensor was embedded into sensor housings and oriented in specific directions. The 1D laser is positioned in such a way that the laser line is aligned with the radial direction of the tire while the 2D laser is positioned in such a way as to cover the largest area of interest. Then the sensor module is mounted on a steel rim by means of tread attachments. A lubricated rubber ring is placed in the groove between two split parts to prevent air leakage. During the measurements, the sensor rotates with the tire and keeps a constant position relative to the objects being measured if the relatively small rim deformation and tire wind-up deformation are neglected.

To measure the angular position of the in-wheel sensor, optical encoders (1024 counts/ revolution, 0.35° resolution for the 1D version and 2048 counts/ revolution, 0.175° resolution for the 2D version) within the slip ring packages were used in the system. In addition, the slip ring packages were also utilized to transmit the multi-channel (10 channels for the 1D version, and 20 channels for the 2D version) analog signals from the in-tire sensor to the data acquisition device through a rotating tire.

The sampling frequencies for the in-tire laser sensors IL-065 and LJ-V7300 were both configured to 3 kHz which implies both are able to measure vibrations of the tire carcass. In this thesis, the excitation during measurements was not

strong enough to fully excite high-frequency vibration modes of the tire carcass. To study the tire in-plane dynamics, additional information on the external excitation and circumferential position of the sensors need to be obtained and synchronized. Moreover, since the internal sensor is fixed to the rim, the update rate for carcass deformation profile is once per rotation. In other words, the spatial resolution of measurement also depends on the rotational velocity. Hence, the exact dynamic measurement ranges at different velocities shall be determined in the future studies.

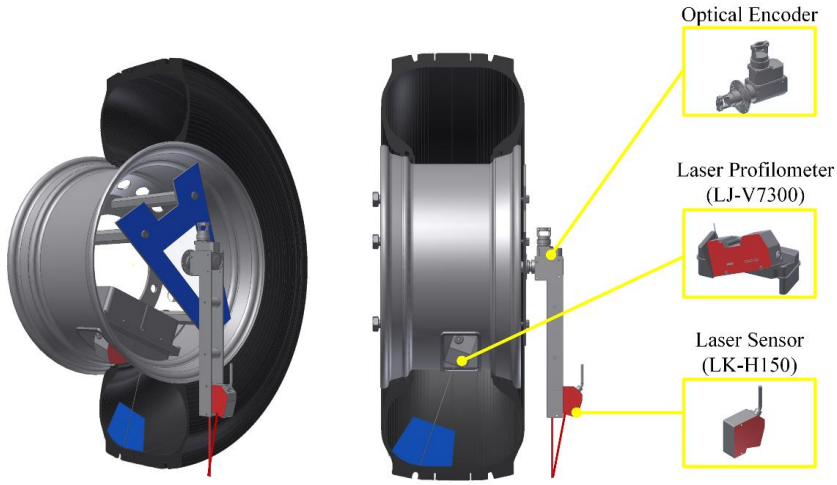

Figure 9 The tread deformation measurement system (2D version).

Since the tread deformation is estimated on the basis of the measurements from several sensors, the synchronization requirement is therefore rigorous. One way of synchronizing the measurements is to generate a trigger signal and connect it to trigger inputs for all sensors. In the 2D system, it is implemented by using the NI module 9474 to generate a pulse train in the data acquisition scheme. In the 1D system, since the laser sensor does not have a triggering function, the delay time was determined experimentally.

3.2 Methodology

From the previous sensor setup, the following quantities were shown to be possible to obtain directly from the sensors, as shown in Figure 10.

- the sidewall height L1:
  the distance from the rim to the inner liner of the tire.
- the loaded radius L2:
  the distance from the axle to the surface of the drum in the vertical direction.
- the circumferential position of the sensor θ:
  the angle θ is defined as the angle between the tire sensor and vertical axis of the tire and 0° is aligned with the six-o'clock position.

In addition, a constant mechanical offset L_{offset}, which is the distance from the starting point of the laser to the rotating axis of the wheel, is measured with a coordinate measuring machine. According to the geometric relationship, the thickness of the tread part under compression could be calculated as:

$$Z_{tread} = L_2 - (L_1 + L_{offset})\cos\theta \tag{3.1}$$

With the original tread thickness known, the tread deflection can be obtained. For measurements conducted on the drum, the curvature of the drum should be considered and Eq. 3.1 should be modified, as demonstrated in Article [I]. It should be noted that the proposed tread deformation measurement should be conducted on a hard and preferably level road surface for free rolling tires in straight-line motion.

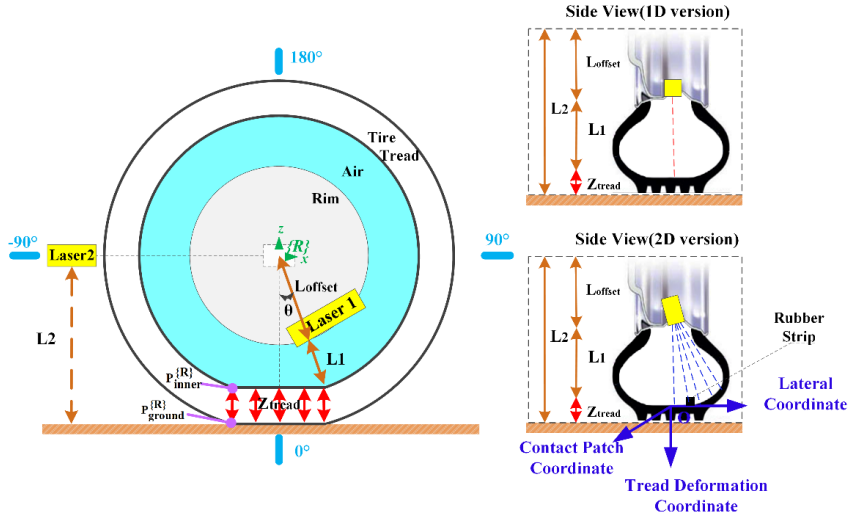

Figure 10. The methodology of tread deformation measurement using optical tire sensors.

For the 2D version of the in-tire sensor, since it was oriented in a specific direction, the measurements in the laser coordinate system needed to be transformed into the defined coordinate system and laser measurement coordinates. In the coordinate transformation, a 9-mm-wide rubber strip was used as a reference object and it was glued to the inner liner and behind a circumferential groove. The rubber strip also allows the possible lateral movement of the tire carcass to be monitored.

In practice, raw signals measured by the sensor cannot be used directly and signal processing is needed. The typical noise in the inner profile measured by the 2D in-tire sensor is outliers, which have unreasonably high and low values compared to the surrounding data. The outliers are caused by the high sampling rate and limited reflectivity of the rubber surface. To eliminate those outliers, a filter based on the cumulative probability neighbor median [47] was used to process the data.

The measurement signals from the external laser include both periodic errors and random noise. The principal cause of the periodic errors was the eccentric alignment between the rotating axes of the tire and slip ring. To reduce such error, a pattern recognition procedure was defined to compensate for it. On the other hand, the random noise from the road roughness (texture less than 1 mm) was smoothed by a Butterworth low-pass filter.

3.3 Measurement environments

Since studies take place under different operational conditions for various purposes, it is important to have controllable environments for measurements on passenger car tires and truck tires with the tire sensor system that was developed.

The measurements of passenger car tires were all conducted on a chassis dynamometer in the vehicle engineering laboratory at Aalto University, Finland (see Figure 11). The test tire was driven by a drum, which was covered with Safety-Walk (roughness of approximately P = 60). The diameter of the drum is 1219 mm, which fulfills the minimum requirement for the drum size, 1200 mm, defined in standards for rolling resistance measurements. The controlled speed is able to reach 200 km/h. Moreover, the test tire could be driven in either the forward or backward direction, which is important for the study of its rolling resistance. The vertical force was adjustable through hydraulic cylinders controlled by p/Q controllers. In addition, different braking forces can be generated with a hydraulic disc brake system, which permits studies on tire braking forces as shown in Article [IV]. To limit the scope of the studies to in-plane tire deformations, the slip and camber angle were both adjusted to 0° in all the studies.

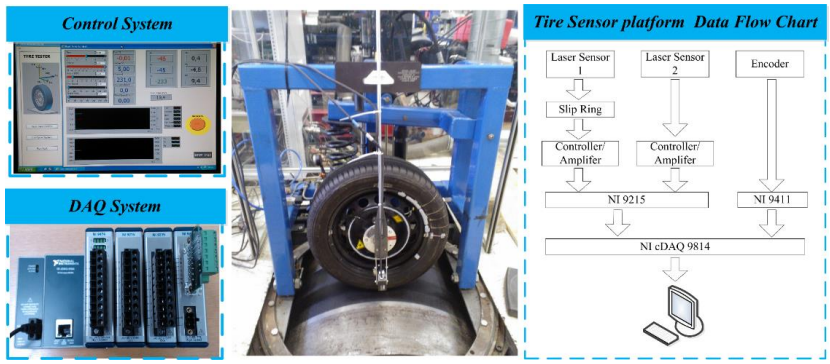

Figure 11 Assembly of the instrumented tire on a chassis dynamometer.

For the measurements with truck tires, a commercial truck (SISU Polar) was used instead of the laboratory test rig, which was designed mainly for passenger car tires. The instrumented tire was assembled onto a lift axle. The experiments were performed in a parking area at Aalto University, Finland, where the cross-section of the road has a crown shape that slopes at 2.6 % on either side of the

road centerlines. Operational factors were controlled as follows. The vertical force applied to the tire being measured was adjusted by alternating the pressure of the air spring. However, it was found that the applied load .The cold inflation pressure was adjusted and checked before each measurement. In all the measurements on free-rolling tires, neither braking nor a drive torque was applied to the wheel. In other words, the slip angle was set to zero and the slip ratio was assumed to be zero. Considering the minor influence of rotation velocity on the rolling resistance at velocities less than 100km/h and the lack of a long enough proving ground, all the experiments were conducted only with one velocity, at 5 km/h.

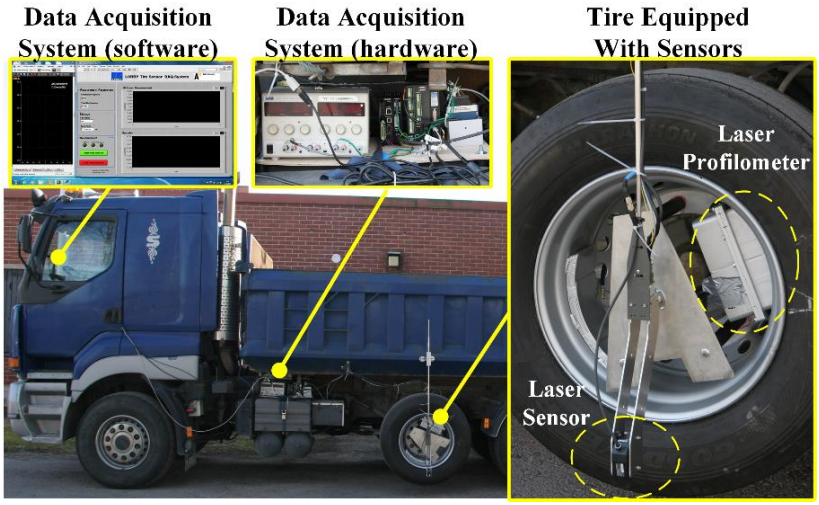

Figure 12 Assembly of the instrumented tire on a truck.

4. Results and discussion

The overall results from the peer-reviewed publications are summarized in this section. A multi-laser tire sensor system (including both 1D and 2D versions) was developed to measure in-plane tire deformations and its methodology was presented (see Articles [I] and [II]). Three physical quantities, namely the tread deformation, carcass deformation, and inner contour of the tire were obtained in measurements with a passenger car tire and truck tires.

For the tread deformation, non-uniform patterns were observed in both the longitudinal and lateral directions (see Articles [I] to [III]). It was found that the asymmetric deformation in the longitudinal direction is linked to the rolling resistance performance of tires. In addition, a load shift effect of the asymmetric deformation was found in the lateral direction.

For the carcass deformation, coupled deformations in the radial and tangential directions were observed (see Article [IV]). It was found that the radial deformation is influenced by both the vertical and longitudinal forces. Indicators based on the radial deformation of the tire carcass were proposed to estimate the in-plane tire forces.

For the partial inner contour, measurements were conducted with a truck tire under static conditions for various inflation pressures and vertical forces.

4.1 Tread deformation

As discussed in Section 2.1.2, highly viscoelastic rubber compounds are commonly used for tread blocks to attain better grip performance. A considerable amount of energy is therefore lost through the cyclic deformation of tread blocks. Hence, tread deformation was one primary physical quantity to be measured in this thesis. The measurements were conducted first with a passenger car tire in a laboratory environment and then with new and used truck tires of the same type on a real truck. In a series of measurements, the deformation of the tread was first investigated on an element located in the middle of the tire crown, and was then extended to a wider area along the tire cross-section.

4.1.1 Non-uniform deformation

The tread deformation in the contact patch was found in measurements to be non-uniform in both the longitudinal and lateral directions. In the longitudinal direction, measurements on a passenger car tire (205/55 R16) revealed an

asymmetric tread deformation in the contact patch for the first time reported in the literature (Article [I]). No matter whether a tire rotated in clockwise or counterclockwise direction, larger deformations were found in the leading half of the contact; meanwhile, smaller deformations were found in the trailing half, as shown in Figure 13. The observed asymmetric deformation of the tread blocks in the longitudinal direction is a direct indicator of the rolling resistance. This statement was also confirmed by the similar asymmetric deformation pattern observed in the measurements with truck tires, as shown in Figure 14.

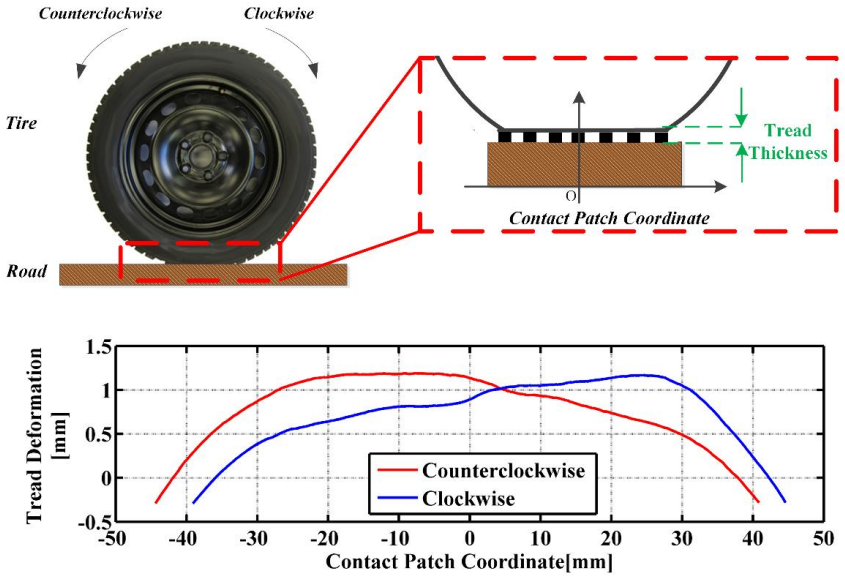

Figure 13 The asymmetric tread deformation for a radial passenger car tire (vertical force=3 kN, velocity=10 kmh^{-1}, and inflation pressure= 2.2 bar).

In measurements with the 2D tire sensor system, the tread deformation was also examined along the lateral direction of the tire cross-section, as shown in Figure 14. It was found that the deformation in the lateral direction is also non-uniform and is strongly influenced by the operational factors and in-service wear of the tire, which will be discussed further in the next two subsections. In addition, the partial tire-road contact patch shape can be obtained from the tread deformation measurements. The evolution of the shape of the contact patch against changes in different operational factors is presented in Article [III].

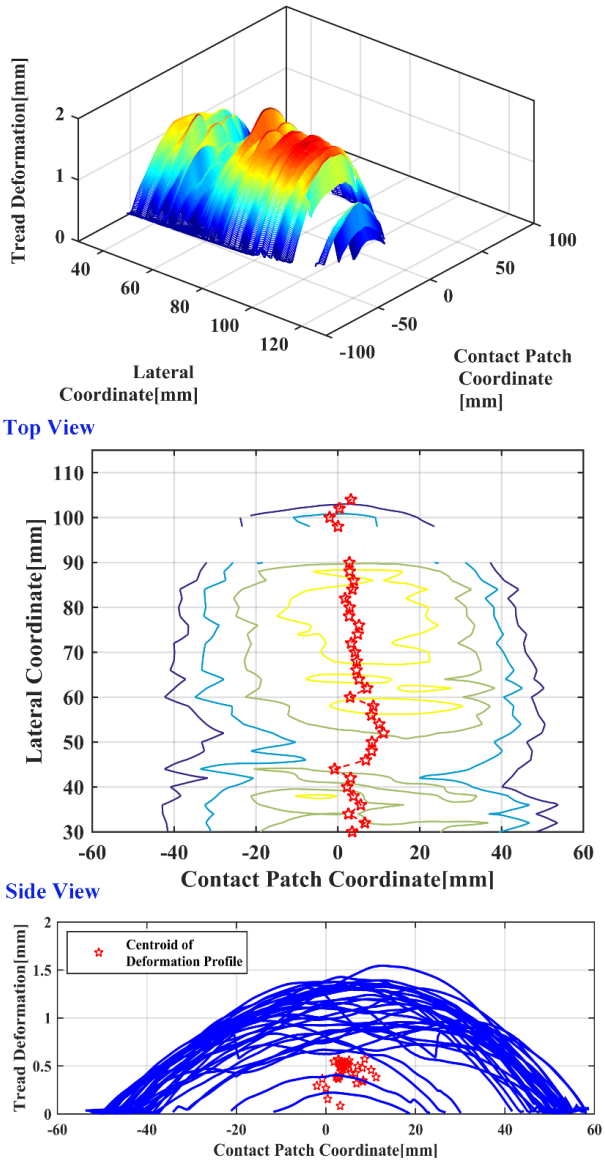

Figure 14 . The measured non-uniform tread deformation for a truck tire (vertical force=25 kN, velocity= 5 kmh^{-1}, and inflation pressure=5.5 bar).

4.1.2 The effect of operational factors

The influences of different operational factors on the tread deformation were investigated with a passenger car tire, as shown in Figure 15 - Figure 17. The measurements suggest that the vertical force and inflation pressure affect the tread deformation considerably, whereas the rolling velocity of the tire in a certain operating range (5-15 km/h), had only a slight effect on the tread deformation.

Under three different vertical forces (2000 N, 4000 N, and 6000 N), the deformation of the tread element appears to be smaller under a higher load, as

shown in Figure 15. This is due to the fact that the location of the tread element is in the middle of the crown, and a so called 'load shift' phenomenon existing in the lateral direction transfers the load from the tire crown to the tire shoulder. However, the load shift phenomenon accompanied by a load increase was not observed within the measurement with the worn truck tire, which will be discussed further.

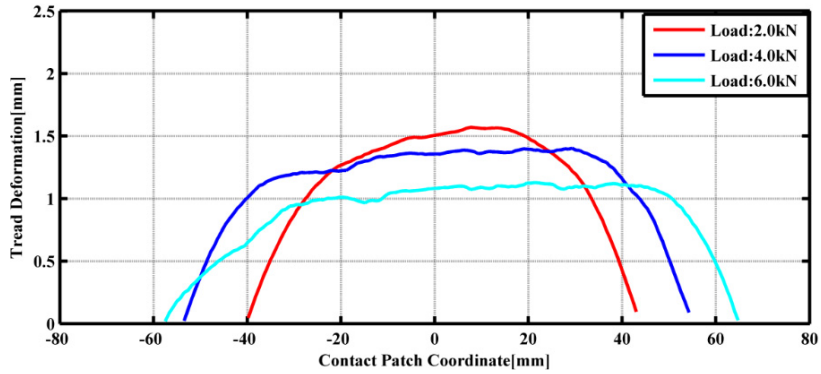

Figure 15 Comparison of the measured tread deformation for a radial passenger car tire under different vertical forces (velocity=5 kmh-1, inflation pressure=2.5 bar).

Figure 16 depicts the tire tread deformation pattern with three different inflation pressures (2.0, 2.5, and 3.0 bar). The comparison indicates that similarly to the load effect, a higher inflation pressure (3.0 bar) will shorten the length of the contact patch. Nevertheless, the magnitudes of the largest deformations do not significantly change with changes in pressure. The same result was observed in [25] for thermal simulations and laboratory measurements. The contribution of the tread to the hysteretic losses is nearly constant with pressure changes. However, the hysteretic losses in other regions, e.g., the shoulder, sidewall, and bead, are more sensitive to changes in the inflation pressure, which leads to the well-known observation that the overall rolling resistance of the tire decreases with increasing inflation pressure.

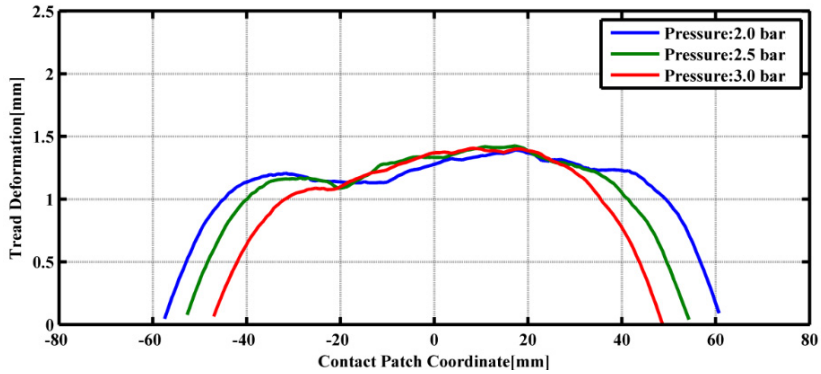

Figure 16 Comparison of the measured tread deformation for a radial passenger car tire at different inflation pressures (vertical force=4 kN, velocity =5 kmh^{-1}).

Figure 17 illustrates the influence of different velocities on tire tread deformation. Five different rotating velocities (5, 8, 10, 13, and 15 km/h) were examined. Compared with the effects from the vertical force, the influence of the velocity is relatively small. There was an observable pattern in the tread deformation shape at different velocities. Moreover, the rotational velocity has a minor effect on the contact length. Similar observations of the velocity on the normal pressure can be found in [22]. These observations agree well with the results and observations in [23], in which the velocity was also shown to have a minor effect on the rolling resistance at velocities less than 100 km/h.

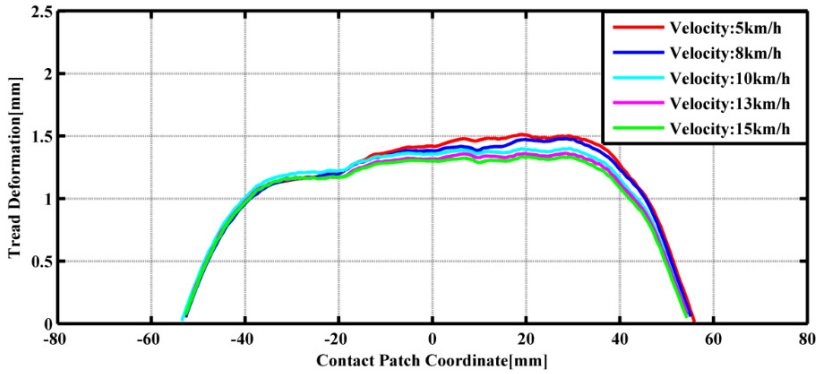

Figure 17 Comparison of the measured tread deformation for a radial passenger car tire at different velocities (vertical force=4 kN, inflation pressure=2.5 bar).

Increases in the rolling velocity also cause the magnitude of the deformation in the leading half to become slightly smaller. The reasons for this phenomenon are probably twofold. On one hand, according to [24], the rubber damping property, which is frequency dependent, might contribute to this effect. On the other hand, the wheel hop caused by the test rig control system might also accounts for the magnitude changes. However, the speed range in 1D measurement has limited to 5-15 km/h. With such a narrow speed range in the experiment, it is difficult to draw general conclusions. Further studies need to be done outside the range of 5-15 km/h.

4.1.3 The effect of wear

In-service wear is an inevitable process that continuously alters the behavior of a tire over its whole lifetime. The influence of tire wear was therefore also investigated on the basis of the measurement of new and worn tires as shown in Figure 18. The load shift phenomenon was observed for the new tire, i.e., the vertical force has an opposite effect on the deformation level in the shoulder part compared to the crown part (Figure 19). The deformation level of shoulder parts increases with an increasing load, whereas the crown parts show an opposite trend. However, no obvious load shift effect were observed on the worn tire (Figure 20). This can mainly be explained by the stiffening of the tread resulting from wear. Moreover, the outer contour of the worn tire also became flattened. It can be seen that the wear effect also has a great influence on the non-uniform

deformation of the tread parts, thus changing the tire crown contour. This in turn accelerates the uneven tread wear [48].

Figure 18 Worn tire and new tire used in the measurement.

According to the measurements in [49], used tires have a generally decreasing trend in rolling resistance with tire usage. This can be related to the measured tread deformation because a worn tire has a smaller tread deformation. Together with a decreasing volume of the tread compound, the observation of a lower rolling resistance with worn tires is expected. Current international standards and labeling regulations only evaluate the rolling resistance performance for new tires. However, the above discussion implies that the rolling resistance performance of the tire during its whole lifetime should also be considered.

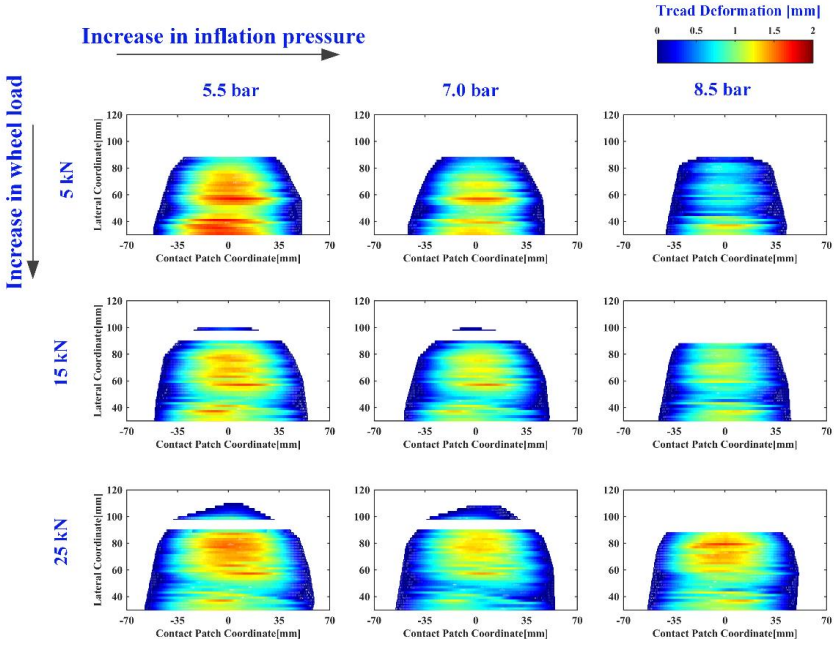

Figure 19 Measured tread deformation of a new tire under various loads and inflation pressure. The white area in the measurements is caused by the rubber strip attached.

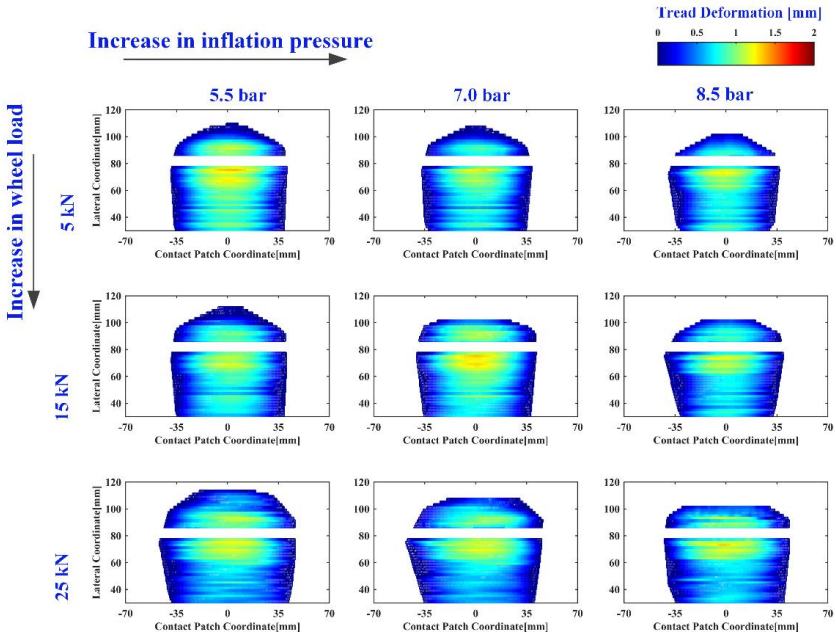

Figure 20 Measured tread deformation of a worn tire under various loads and inflation pressures. The white area in the measurements is caused by the rubber strip attached.

4.2 Carcass deformation

Although the carcass deformation was previously measured in [41]–[44], the potential to use that information to estimate tire forces has not been fully explored. This study focuses on the analysis of the deformation of the tire carcass as a result of the applied steady-state in-plane tire forces and proposes two indicators to correlate the radial deformation of the tire carcass with in-plane tire forces.

The simulations with the flexible ring tire model were conducted with various vertical forces and inflation pressures to analyze their influences on the in-plane tire deformation, as shown in Figure 21.

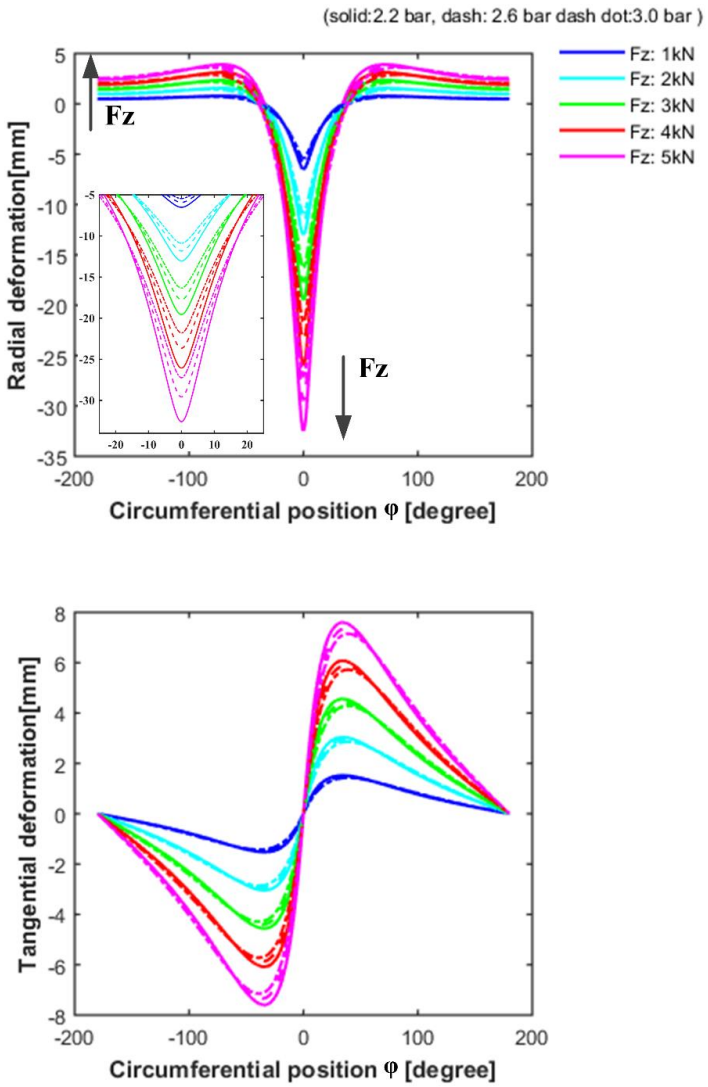

Figure 21 Simulated in-plane tire deformations under different vertical forces: (a) radial deformations and (b) tangential deformations.

To validate the simulation results, the radial deformation of tire carcass was measured with the in-tire laser sensor under various vertical force, as shown in Figure 22. The same behavior can be found between the simulations and measurements. The deformation can be further divided into two areas: the contact zone and non-contact zone. It is found that the deformation peaks occur during the contact between the tire and road, and the largest deformation is obtained at the highest load. On the other hand, the radius of the non-contact zone becomes larger with increasing loads. This is due to the high extensional stiffness of the tire belt for a radial tire, which is almost in-extensible. Moreover, the volume of pressurized air does not change with increasing loads which also results in the non-contact parts being pushed outwards in the radial direction.

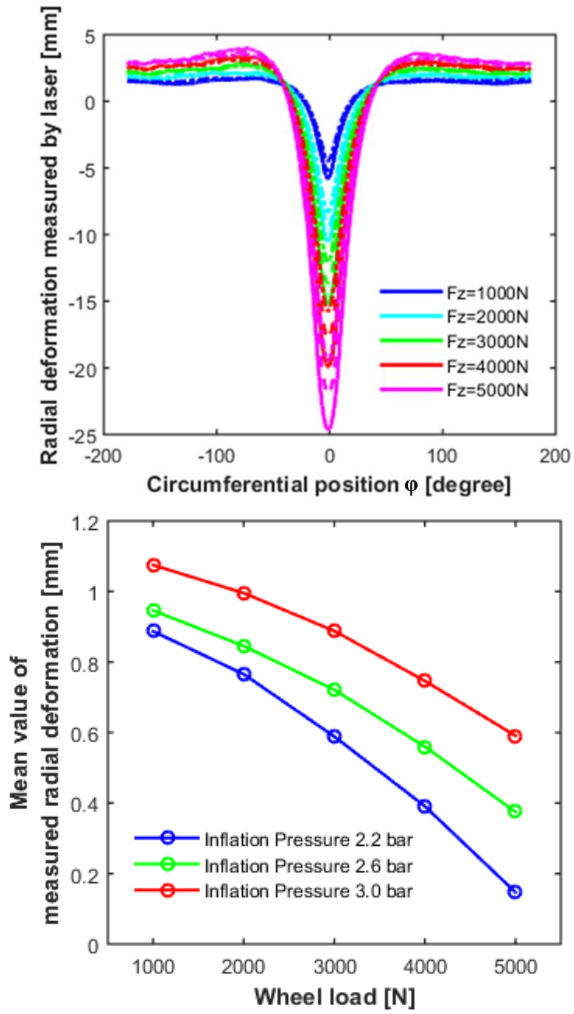

Figure 22 Measured radial deformations of the tire under different vertical forces (*Fx*: 0 N, inflation pressure: 2.6 bar) and at various inflation pressures (solid line: 2.2 bar, dashed line: 2.6 bar, and dashed-dotted line: 3.0 bar).

To correlate the radial deformation of the tire carcass to the vertical forces applied, the measured radial deformations with angular positions were first interpolated to 1000 equidistant circumferential positions between -180° and 180°. The mean radial deformation value w_{l_m}, as an indicator, is calculated as follows:

$$w_{l\_m} = \sum w_{laser}(\varphi, -180° \le \varphi \le 180°)/N \tag{4.1}$$

where $w_{laser}(\varphi)$ is the interpolated radial deformation at a specific circumferential position φ. In other words, the mean radial deformation is an average of the tire deformations in one full rotation, which include two deformations, the inward radial deformation resulting from the tire-road contacts and the outward radial deformation resulting from the tire structures. The mean radial deformation is plotted against the vertical forces and

demonstrates a near-linear relationship for all the pressures that were applied. It can be seen that the inflation pressure has a significant influence on the radial stiffness, in addition to the contribution of the tire structure. In both the high load and low inflation pressure cases, the observed smaller mean deformation values imply larger inward deformations (with a negative value) in the tire-road contact.

The radial deformation of the tire carcass was also measured with the in-tire laser sensor under various vertical forces, as shown in Figure 23. The symmetricity of the radial deformation of the tire changes with the longitudinal force that is applied as a result of the pretension force and inextensibility of the ring structure. In addition, the simulation results with the flexible ring tire model are similar to the measurements obtained with the tire sensors, as shown in Figure 24. In previous studies [41], [42], the longitudinal force was estimated on the basis of separate measurements of the longitudinal deformation of the tire carcass. However, the present study suggests that the longitudinal force can also be estimated on the basis of measurements of radial deformations.

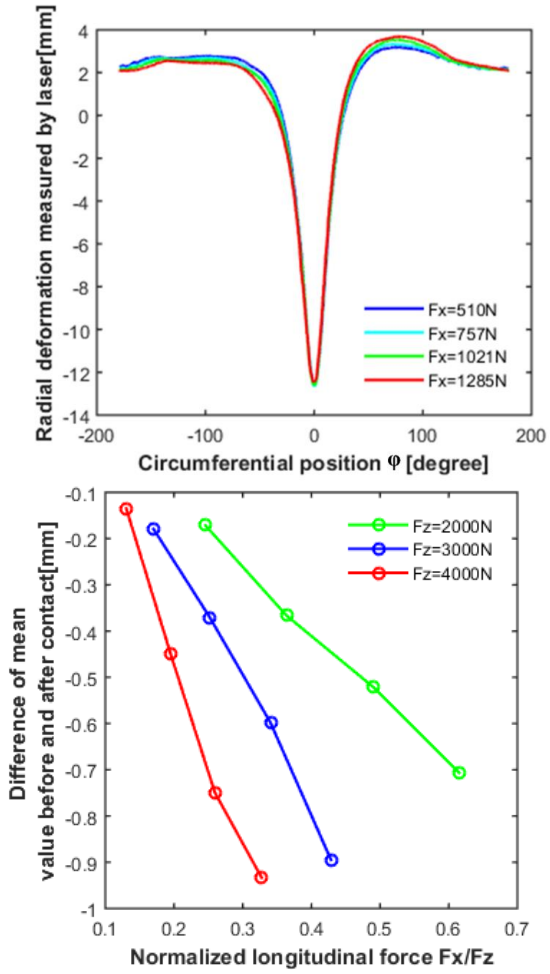

Figure 23 Measured tire radial deformation under different longitudinal forces (*Fz*: 3000 N and inflation pressure: 2.6 bar).

As a simple indicator, such asymmetricity can be measured by the difference between the mean measured deformation values before and after the contact, w_{l_d}, which can be calculated as follows:

$$w_{l\_d} = 2\left\{\sum w_{laser}(\varphi, -180° \le \varphi \le 0°) - \sum w_{laser}(\varphi, 0° \le \varphi \le 180°)\right\}/N \quad (4.2)$$

The calculated mean value differences with negative values imply that the tire has a smaller radius before the tire-road contact. As shown in Figure 23, the mean value difference has a linear relationship with the longitudinal forces and shows a dependence on the vertical force. The difference is larger at a higher load condition.

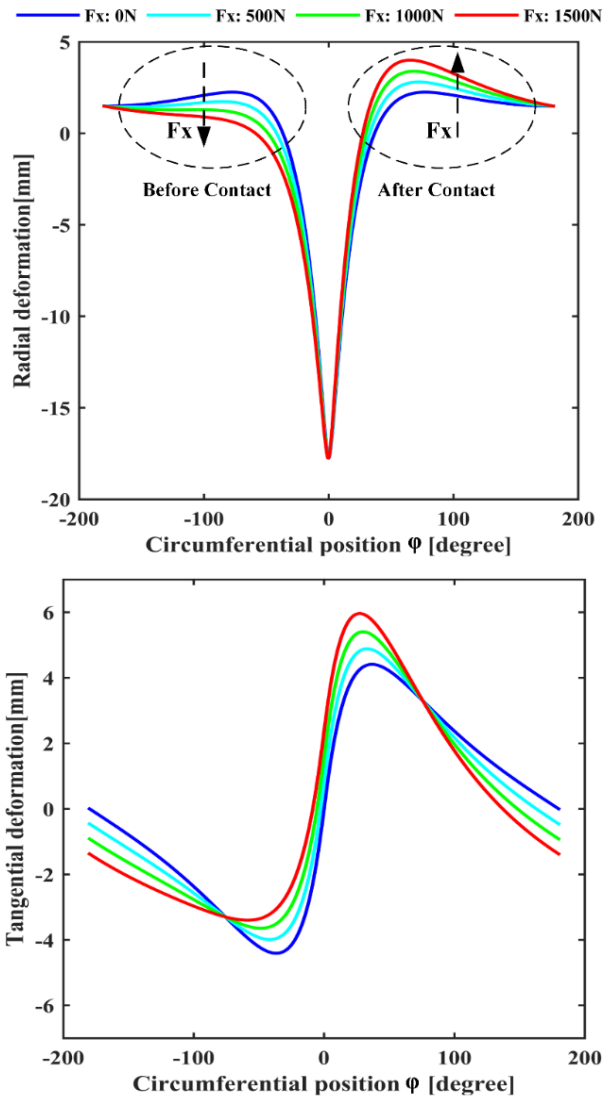

Figure 24 Simulated in-plane tire deformations under different longitudinal forces: (a) radial deformations and (b) tangential deformations (*Fz*: 3000 N and inflation pressure: 2.6 bar).

The proposed indicator allows the estimation of the longitudinal force to be based solely on the measurement of the radial carcass deformation. This demonstrates the feasibility to use the tire carcass deformation for the in-plane tire force estimation. It should also be noted that this feature-based indicator is relatively simple and cannot be used directly for real on-board applications. One promising approach is using a model-based approach that utilizes the carcass deformation as an input for the flexible ring tire model to identify the input tire forces. However, the accuracy of such estimator highly depends on the fidelity of parameters of the flexible ring tire model. These parameters can be influenced by the tire inflation pressure, tire rotational velocity, and tire wear.

4.3 Inner contour

Pneumatic tires have a complex composite structure with a doubly curved surface, which is curved both circumferentially and transversely. The tire contour has a direct influence on the performance of the vehicle such as the smoothness of the ride and the ease of its handling. The shape of the contour is optimized with finite element models (FEM) to improve the tire performance after inflation and under loads. Current tire crown optimization approaches, such as the tension control optimization theory (TCOT), aim to improve the tension distribution within the parts of the tire. Direct measurements of the shape of the tire inner contour are desired, as this reflects the tension distribution. However, the actual shape of the tire contour is rarely measured through experiments, because of the lack of a simple and cost-effective method. The laser-based tire sensor system provides an opportunity to measure the inner contour of the tire under both static and dynamic conditions.

Measurements were conducted under static conditions for various inflation pressures and vertical forces. To examine the influence of the tire inflation pressure, the inner contours were measured at 2 bar, 4 bar, and 6 bar. As shown in Figure 25, increasing the inflation pressure results in the tire carcass being pushed outwards in the radial direction. Moreover, prominent changes were observed in the shoulder part and the sidewall curvature radius decreased slightly with an increase in the inflation pressure. According to the membrane theory, the sidewall tension is directly proportional to the sidewall curvature radius. In a different manner, increasing the vertical force leads to the crown part moving in the vertical direction and a remarkable decrease in the sidewall curvature radius. This implies a tension relaxation process in the tire-road contact for a rolling tire discussed in [10].

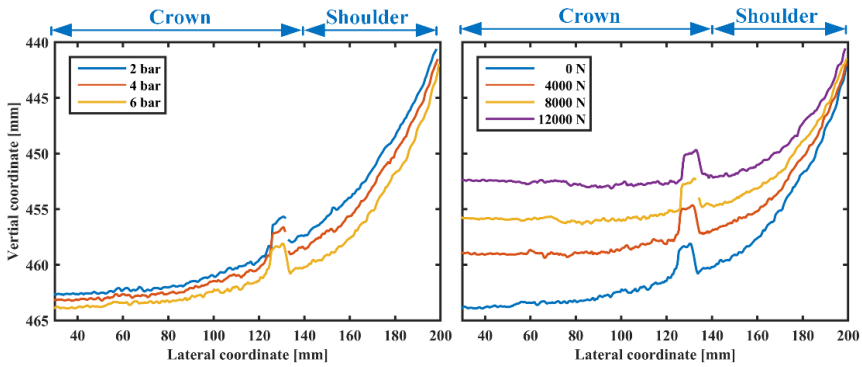

Figure 25 Measured tire inner contours under various inflation pressures (under a zero vertical force) and various vertical forces (with a 4 bar inflation pressure).

The inner contour was also measured under service conditions. To reconstruct the inner contour of the tire during rolling, the 2D laser profilometer needs to rotate together with a tire for at least one revolution. The measured inner contour shows two-phase deformations experienced by a tire in each revolution: the contact deformation (from around -40 degrees to around 40 degrees) and the non-contact deformation (for the remaining parts of the measurement), as shown in Figure 26 (a). The contact deformation, with a larger amplitude, is a result of tire-road contacts and is mainly influenced by the vertical force and vertical stiffness of the tire. Over the tire cross-section, the system can examine tire deformation over a larger area including parts of the shoulder and crown. Within the contact patch, parts of the tire along the lateral direction show a non-uniform contact deformation. For a better visualization, the measured tire inner contour is also depicted in the polar coordinates, as shown in Figure 26 (b).

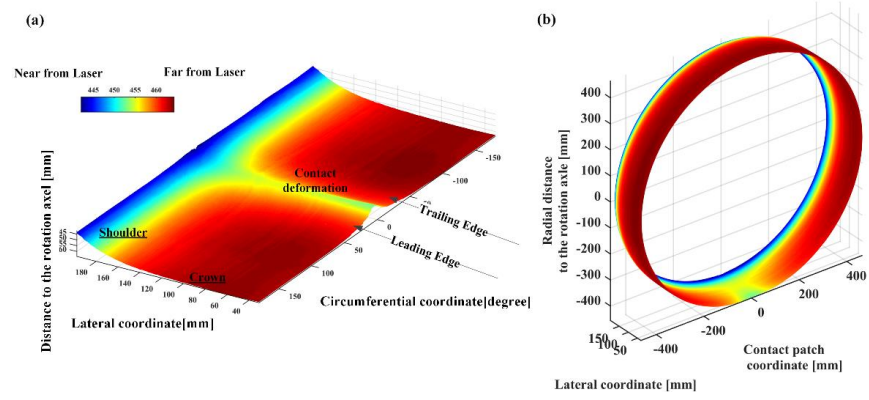

Figure 26 Measured inner contours of the tire for one revolution: (a) in Cartesian coordinates; (b) in polar coordinates.

5. Conclusions

In-plane tire deformations are a direct result of the in-plane forces applied to a tire. Therefore, the in-plane deformations in different parts of the tire contain unique information about tire forces. For instance, deformations in the tread part are closely related to the rolling resistance performance. On the other hand, deformations in the carcass part are strongly influenced by the vertical force and longitudinal forces.

Tire sensing technology provides an opportunity to measure those deformations accurately. A multi-laser tire sensor system was developed to measure rolling tire deformations, including the tread deformation, carcass deformation, and the shape of inner contour. The structure and methodology of the tire sensor system are presented in detail. In the context of different tire performances, in-plane tire deformations were measured and analyzed with different tire types, operational conditions, and tire states.

Tread deformation measurements were carried out, with the main interest being in investigating its correlation with the rolling resistance. The test matrices incorporate different potential influential factors, which are tire types, namely the passenger car and truck tires, tire states, namely the new and used tires, and operational conditions, namely the pressures, loads, and velocities. Some common phenomena can be observed from the measurements and summarized as follows.

First and foremost, non-uniform tread deformations in the contact patch were observed in the measurements. In the longitudinal direction, larger tread deformations were observed in the leading half of the contact patch, while smaller tread deformations were observed in the trailing half of the contact patch. This is a direct indicator of the rolling resistance and is observed in most measurements. In the lateral direction, non-uniform deformations were also observed. The deformation pattern reflects the contribution of separate parts to the rolling resistance.

In addition, the non-uniformity of the tread deformation is also strongly influenced by operating conditions and tire states. It is found that the tire inflation pressure and vertical force have significant influences on the tread deformation pattern, while the velocity, in a certain range (5-15 km/h), shows a minor influence. In the lateral direction, for new tires, the measurements indicate a load shift phenomenon, i.e., the largest tread deformation shifts from the crown parts to the shoulder parts under an increasing vertical force.

Nevertheless, this phenomenon is not observed in worn tires. This is related to tire wear in the crown part, in which a flatter contour can be found.

In view of the above, it can be concluded that the rolling resistance performance can be improved through the optimization of tire design and material, as well as the maintenance of proper operational conditions, especially the inflation pressure. In addition, an evaluation standard which incorporates the whole-life time rolling resistance performance of tires should be considered in the future.

Carcass deformation measurements were also conducted, with the main interest being in the estimation of the tire forces. It was found that the radial deformation can be used not only to estimate vertical tire loads, but also to estimate longitudinal forces, such as braking and acceleration forces. For vertical force estimations, the average of radial deformation is proposed as an indicator. On the other hand, the longitudinal force can be estimated on the basis of the symmetricity of the radial deformation of the carcass. The physical foundation of this algorithm is the extensibility of the modern radial tire, in which the radial and tangential deformations of the carcass are cross-correlated. The simulation results with the flexible ring tire model confirmed this.

The partial inner contour was also measured for truck tires under static conditions for various inflation pressures and vertical forces. The measurements can provide valuable experimental information about tire products for tire designers to optimize tire contours.

In conclusion, the tire-sensing technology provides promising solutions in two major fields: 1) measuring tire behavior, and 2) sensing tire forces. In this thesis, the measurements of tread deformations and inner contours are examples that fall into the first category. Meanwhile, measurements of radial deformation of the tire carcass for estimations of steady-state in-plane tire forces represent an example of the second category. In future, with the advance of sensing technology and deeper understanding of tire behavior, it is believed that the tire sensor system will be able to provide more accurate and real-time information on tire-road interactions.

References

[1] "ETRMA Annual Report 2013/2014," European Tyre Rubber Manufactures Association, Brussels, 2014.

[2] E. Pike, "Opportunities to Improve Tire Energy Efficiency," The International Council on Clean Transportation, Washington, D.C., 2011.

[3] European Union Parliament, "Regulation (EC) No 1222/2009 of the European Parliament and of the Council of 25 November 2009 on the Labelling of Tyres with Respect to Fuel Efficiency and Other Essential Parameters," 2009.

[4] European Commission, "Roadmap to a Single European Transport Area– Towards a Competitive and Resource Efficient Transport System," White Paper, Communication 144, 2011.

[5] "Multiannual Roadmap for the Contractual Public Private Partnership 'European Green Vehicles Initiative,'" The European Road Transport Research Advisory Council, Brussels, 2013.

[6] "Tires and Passenger Vehicle Fuel Economy," Transportation Research Board of the National Academies, Washington, D.C., 2006.

[7] K. Holmberg, P. Andersson, N. O. Nylund, K. Mäkelä, and A. Erdemir, "Global energy consumption due to friction in trucks and buses," Tribol. Int., vol. 78, pp. 94–114, 2014.

[8] K. Holmberg, P. Andersson, and A. Erdemir, "Global energy consumption due to friction in passenger cars," Tribol. Int., vol. 47, pp. 221–234, 2012.

[9] R. Moser and J. G. Lightner, "Using three-dimensional digital imaging correlation techniques to validate tire finite-element model," Exp. Tech., vol. 31, no. 4, pp. 29–36, Jul. 2007.

[10] A. N. Gent and J. D. Walter, The Pneumatic Tire. The National Highway Traffic Safety Administration, Washington, D.C., 2005.

[11] S. Clark, Mechanics of Pneumatic Tires. U.S. Department of Transportation, The National Highway Traffic Safety Administration, Washington, D.C., 1981.

[12] J. D. Ferry, Viscoelastic Properties of Polymers. John Wiley & Sons, 1980.

[13] S. Mihara, "Reactive processing of silica-reinforced tire rubber: new insight into the time- and temperature-dependence of silica rubber interaction," Ph.D. Dissertation, University of Twente, 2009.

[14] B. N. J. Persson, Sliding Friction: Physical Principles and Applications. Springer Science & Business Media, 2000.

[15] P. E. Austrell and A. K. Olsson, "Modelling procedures and properties of rubber in rolling contact," Polym. Test., vol. 32, no. 2, pp. 306–312, 2013.

[16] M. M. Davari, J. Jerrelind, A. Stensson Trigell, and L. Drugge, "A multi-line brush based tyre model to study the rolling resistance and energy loss," in Proceedings of 4th International Tyre Colloquium: Tyre Models for Vehicle

Dynamics Analysis, Guildford, UK, 2015.

[17] S. Boere, I. L. Arteaga, A. Kuijpers, and H. Nijmeijer, “Tyre/road interaction model for the prediction of road texture influence on rolling resistance,” Int. J. Veh. Des., vol. 65, no. 2-3, p. 202, 2014.

[18] M. Fraggstedt, “Vibrations, damping and power dissipation in car tyres,” Ph.D. Dissertation, Royal Institute of Technology, TRITA-AVE 2008:24, 2008.

[19] L. R. Evans, J. D. MacIsaac Jr., J. R. Harris, K. Yates, W. Dudek, J. Holmes, D. J. Popio, D. Rice, and D. M. K. Salaani, “NHTSA Tire Fuel Efficiency Consumer Information Program Development: Phase 2 – Effects of Tire Rolling Resistance Levels on Traction, Tread wear, and Vehicle Fuel Economy,” The National Highway Traffic Safety Administration, Washington, D.C., 2009.

[20] H. B. Pacejka, Tire and Vehicle Dynamics, 3rd ed. Elsevier, 2012.

[21] Y. Xiong, Y. Zhuang, and A. J. Tuononen, “Assessment of brush model based friction estimator using lateral vehicle dynamics,” in The 12th International Symposium on Advanced Vehicle Control (AVEC), Tokyo, Japan, 2014.

[22] I. J. M. Besselink, A. J. C. Schmeitz, and H. B. Pacejka, “An improved Magic Formula/Swift tyre model that can handle inflation pressure changes,” Veh. Syst. Dyn., vol. 48, no. 1, pp. 337–352, 2010.

[23] P. Zegelaar, “The dynamic response of tyres to brake torque variations and road unevennesses,” in SAE Technical Paper, 1998.

[24] P. Kindt, P. Sas, and W. Desmet, “Measurement and analysis of rolling tire vibrations,” Opt. Lasers Eng., vol. 47, no. 3–4, pp. 443–453, Mar. 2009.

[25] C. Hoever, “The simulation of car and truck tyre vibrations, rolling resistance and rolling noise,” Ph.D. Dissertation, Chalmers University of Technology, ISBN: 978-91-7597-056-1, 2014.

[26] S. Gong, “A study of in-plane dynamics of tires,” Ph.D. Dissertation, Delft University, 1993.

[27] Y. T. Wei, L. Nasdala, and H. Rothert, “Analysis of forced transient response for rotating tires using REF models,” J. Sound Vib., vol. 320, no. 1–2, pp. 145–162, 2009.

[28] C. Wang, B. Ayalew, T. Rhyne, S. Cron, and B. Dailliez, “Static analysis of a thick ring on a unilateral elastic foundation,” Int. J. Mech. Sci., vol. 101–102, pp. 429–436, 2015.

[29] “Intelligent Tyre Systems - State of the Art and Potential Technologies,” APOLLO Deliv D7 Proj. IST- 2001–34372, Apollo Consortium, 2003.

[30] R. Matsuzaki and A. Todoroki, “Wireless monitoring of automobile tires for intelligent tires,” Sensors, vol. 8, no. 12, pp. 8123–8138, Dec. 2008.

[31] S. C. Ergen, A. Sangiovanni-Vincentelli, X. Sun, R. Tebano, S. Alalusi, G. Audisio, and M. Sabatini, “The tire as an intelligent sensor,” IEEE Trans. Comput. Des. Integr. Circuits Syst., vol. 28, no. 7, pp. 941–955, 2009.

[32] T. Becherer, “The sidewall torsion sensor system,” in Darmstädter Reifenkolloquium, pp. 130–137, 1998.

[33] A. J. Tuononen, “Laser triangulation to measure the carcass deflections of a rolling tire,” Meas. Sci. Technol., vol. 22, no. 12, 15304, 2011.

[34] O. Yilmazoglu, M. Brandt, J. Sigmund, E. Genc, and H. L. Hartnagel, "Integrated InAs/GaSb 3D magnetic field sensors for 'the intelligent tire,'" Sensors and Actuators A: Physical, vol. 94. pp. 59–63, 2001.

[35] A. J. Niskanen and A. J. Tuononen, "Three 3-axis accelerometers fixed inside the tyre for studying contact patch deformations in wet conditions," Veh. Syst. Dyn., vol. 52, no. sup1, pp. 287–298, Mar. 2014.

[36] Y. Zhang, J. Yi, and T. Liu, "Embedded flexible force sensor for in-situ tire–road interaction measurements," IEEE Sens. J., vol. 13, no. 5, pp. 1756–1765, 2013.

[37] H. Morinaga, Y. Wakao, Y. Hanatsuka, and K. Akira, "The possibility of intelligent tire (technology of contact area information sensing)," in FISITA World Automotive Congress, 2006.

[38] V. D'Alessandro, S. Melzi, M. Sbrosi, and M. Brusarosco, "Phenomenological analysis of hydroplaning through intelligent tyres," Veh. Syst. Dyn., vol. 50, no. sup1, pp. 3–18, 2012.

[39] M. Matilainen and A. Tuononen, "Tyre contact length on dry and wet road surfaces measured by three-axial accelerometer," Mech. Syst. Signal Process., vol. 52–53, pp. 548–558, 2015.

[40] M. Brandt, V. Bachmann, A. Vogt, M. Fach, K. Mayer, B. Breuer, and H. L. Hartnagel, "Highly sensitive AIGaAs/GaAs position sensors for measurement of tyre tread deformation," Electron. Lett. , vol. 34, no. 8, pp. 760–762, 1998.

[41] A. J. Tuononen, "On-board estimation of dynamic tyre forces from optically measured tyre carcass deflections," International Journal of Heavy Veh. Syst., vol. 16.pp.362-378, 2009.

[42] A. J. Tuononen, "Optical position detection to measure tyre carcass deflections," Veh. Syst. Dyn., vol. 46, no. 6, pp. 471–481, 2008.

[43] A. J. Tuononen and L. Hartikainen, "Optical position detection sensor to measure tyre carcass deflections in aquaplaning," Int. J. Veh. Syst. Model. Test., vol. 46, pp. 471–481, 2008.

[44] S. D. Naranjo, C. Sandu, S. Taheri, and S. Taheri, "Experimental testing of an off-road instrumented tire on soft soil," J. Terramechanics, vol. 56, pp. 119–137, Dec. 2014.

[45] R. Matsuzaki, N. Hiraoka, A. Todoroki, and Y. Mizutani, "Optical 3D deformation measurement utilizing non-planar surface for the development of an 'intelligent tire,'" J. Solid Mech. Mater. Eng., vol. 4, no. 4, pp. 520–532, 2010.

[46] G. Erdogan, L. Alexander, and R. Rajamani, "Estimation of tire-road friction coefficient using a novel wireless piezoelectric tire sensor," IEEE Sens. J., vol. 11, no. 2, pp. 267–279, Feb. 2011.

[47] M. F. Ismail, K. Yanagi, and A. Fujii, "An outlier correction procedure and its application to areal surface data measured by optical instruments," Meas. Sci. Technol., vol. 21, no. 10, 105105, Oct. 2010.

[48] J. R. Cho, S. W. Shin, and W. S. Yoo, "Crown shape optimization for enhancing tire wear performance by ANN," Comput. Struct. , vol. 83, no. 12–13, pp. 920–933, May 2005.

[49] J. R. Luchini, M. M. Motil, and W. V. Mars, "Tread depth effects on tire rolling resistance," Tire Sci. Technol., vol. 29, no. 3, pp. 134–154, Jul. 2001.

Errata

Article [III]

In Section 3.2.3, it should read ‘In-service wear is an inevitable process…’.

In Table 1, the contact area for the condition 8.5 bar and 5 kN is ‘41.5 cm^2’ and the contact area for the condition 8.5 bar and 25 kN is ‘51.7 cm^2’.

Article [IV]

In Figure 2, the horizontal label should read ‘Circumferential position φ [degree]’.

In Figure 3, the horizontal label should read ‘Circumferential position φ [degree]’.

Aalto-DD 89/2016

ISBN 978-952-60-6802-2 (printed)
ISBN 978-952-60-6803-9 (pdf)
ISSN-L 1799-4934
ISSN 1799-4934 (printed)
ISSN 1799-4942 (pdf)

Aalto University
School of Engineering
Department of Mechanical Engineering
www.aalto.fi

BUSINESS +
ECONOMY

ART +
DESIGN +
ARCHITECTURE

SCIENCE +
TECHNOLOGY

CROSSOVER

**DOCTORAL
DISSERTATIONS**